Tue Thur
13:00-14:15 (S103)

UNIST

AMS43101

(Introduction to) Magnetic properties of materials

Ch. 7 Micromagnetism, domains and hysteresis

Ki-Suk Lee

Class Lab.

Materials Science and Engineering

Nano Materials Engineering Track

Creative Lab. for
Advanced Spin System

Goal of chapter 7

The **domain structure** of ferromagnets and ferrimagnets is a result of minimizing the free energy, which includes a self-energy term due to the dipole field $H_d(r)$.

Free energy in **micromagnetic theory** is expressed in the continuum approximation, where atomic structure is averaged away and $M(r)$ is a smoothly varying function of constant magnitude.

Domain formation helps to minimize the energy in most cases.

The **Stoner–Wohlfarth model** is an exactly soluble model for coercivity based on the simplification of coherent reversal in single-domain particles.

The concepts of **domain-wall pinning** and **nucleation of reverse domains** are central to the explanation of coercivity in real materials.

The magnetization processes of a ferromagnet are related to the modification, and eventual elimination of the domain structure with increasing applied magnetic field.

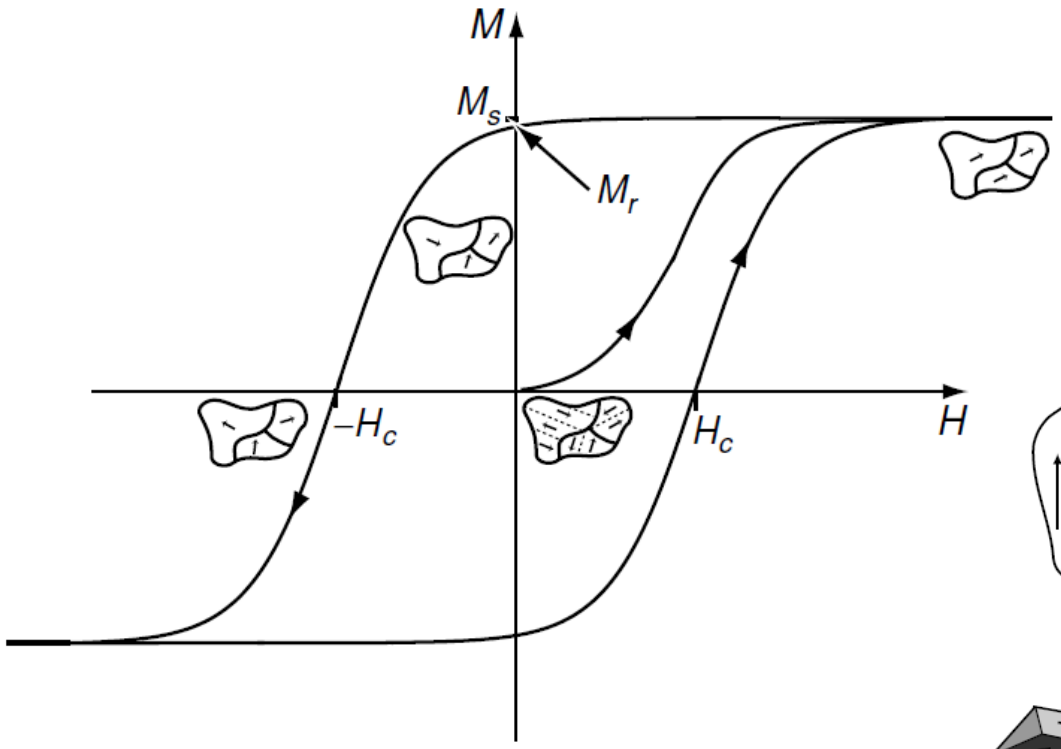

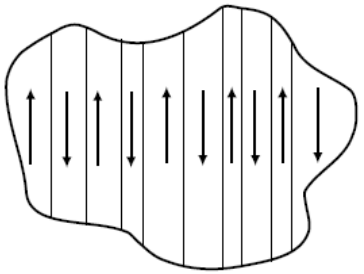

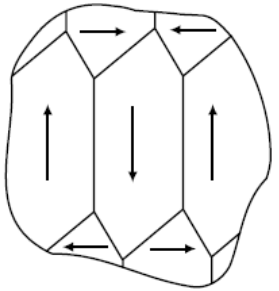

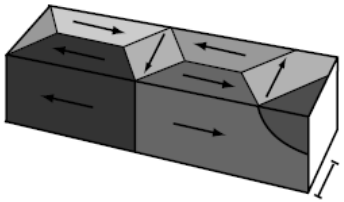

(a)

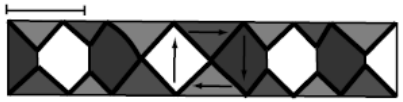

(b)

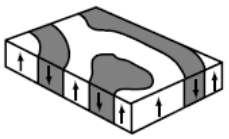

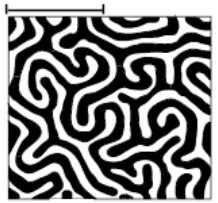

Micromagnetic simulation

A continuum theory for describing the magnetic phenomena

Governing equation:

Landau-Lifshitz-Gilbert (LLG)

$$\frac{d\mathbf{M}}{dt} = -\gamma(\mathbf{M}\times\mathbf{H}_{eff}) + \frac{\alpha_G}{M_S}\left[\mathbf{M}\times\frac{d\mathbf{M}}{dt}\right]$$

$\mathbf{H}_{eff} \equiv \frac{\delta E}{\delta \mathbf{M}}$, functional derivative of the energy

$$E = E_{exch} + E_d + E_{zeeman} + E_{ani}$$

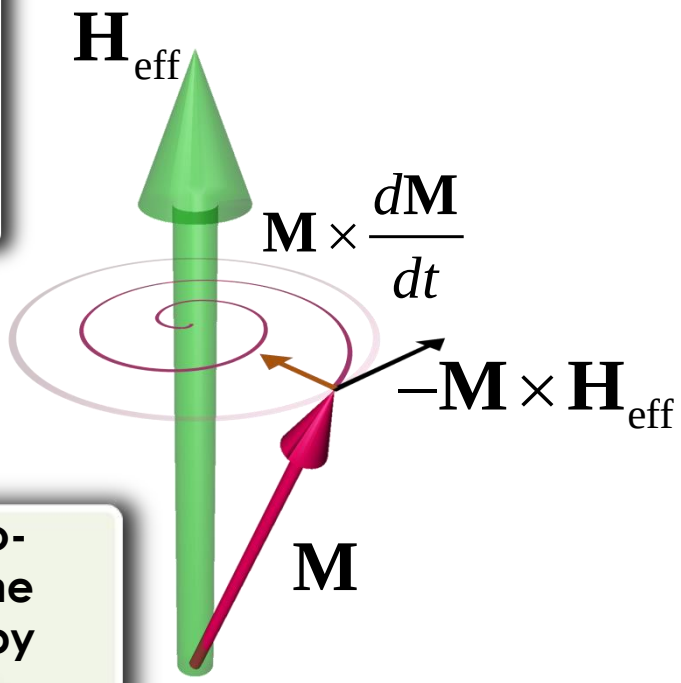

Exchange coupling

Dipole-dipole interaction

Zeeman

Magneto-cryatalline Anisotropy

The basic premise of micromagnetism is that

- A magnet is a mesoscopic continuous medium where atomic-scale structure can be ignored (§2.1): $M(r)$ and $H_d(r)$ are generally nonuniform, but continuously varying functions of r.
- $M(r)$ varies in direction only: its magnitude is the spontaneous magnetization M_s .

Domains tend to form in the lowest-energy state of all but submicrometre-sized ferrromagetic or ferrimagnetic samples, because the system wants to minimize its total self-energy, which can be written as a volume integral of the energy density E_d , in terms of the demagnetizing field (2.78):

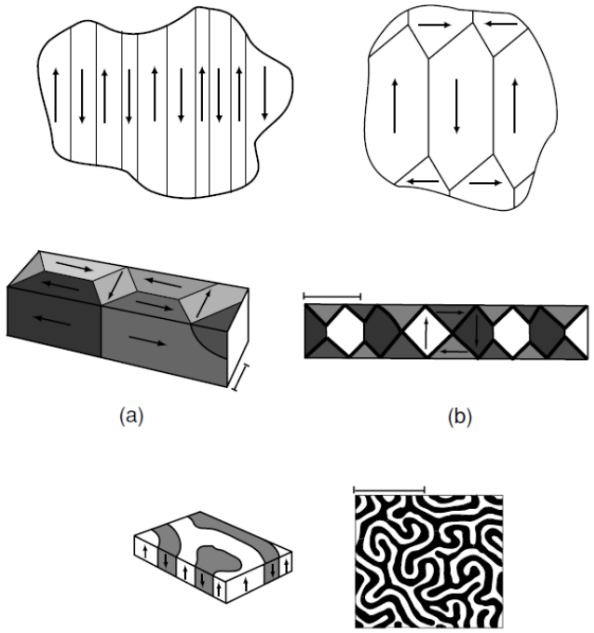

$$\varepsilon_d = -\frac{1}{2}\int \mu_0 \boldsymbol{H}_d \cdot \boldsymbol{M}\,\mathrm{d}^3 r.$$

Energy minimization is subject to constraints imposed by exchange, anisotropy and magnetostriction.

The domain structure is eliminated by a large-enough applied field, and the underlying spontaneous magnetization of the ferromagnet is then revealed.

On reducing the field, a new domain structure forms and hysteresis appears.

The hysteretic response of a ferromagnet, like the behaviour of a person, depends not only on current circumstances but on what has gone before.
Magnets have memory.

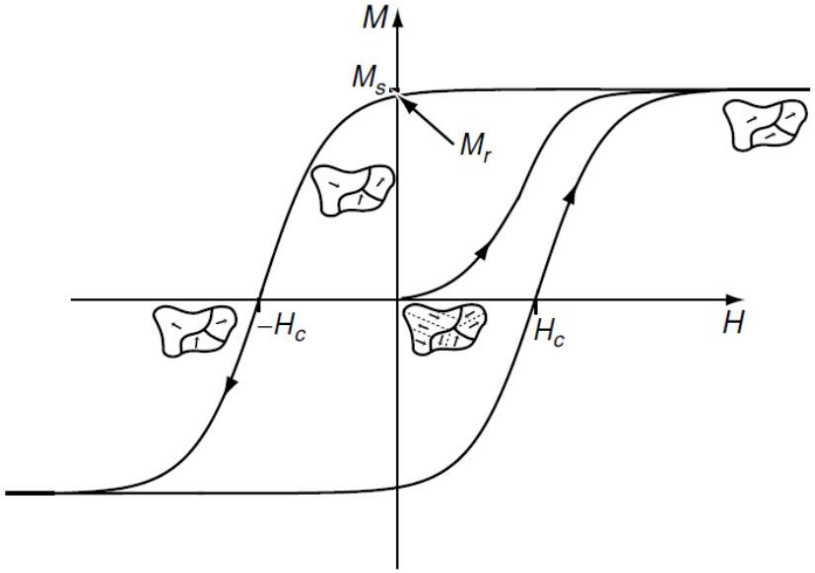

Demagnetizing fields and stray fields arise whenever the magnetization has a component normal to an external or internal surface. They also arise whenever the magnetization is nonuniform in such a way that

$$\nabla \cdot \boldsymbol{M} \neq 0.$$

The direction of magnetization in a domain is mainly governed by magnetocrystalline anisotropy, so a stray field associated with surface 'charge' density

$$\sigma = \boldsymbol{M} \cdot \mathbf{e}_n$$

may be created at surfaces which do not lie parallel to the easy axis of uniaxial magnets (2.54).

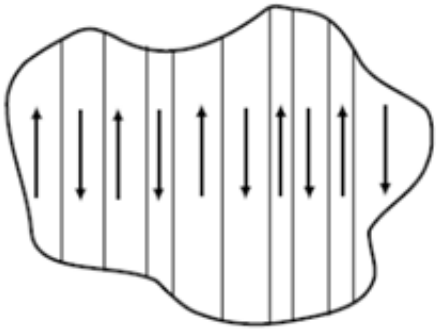

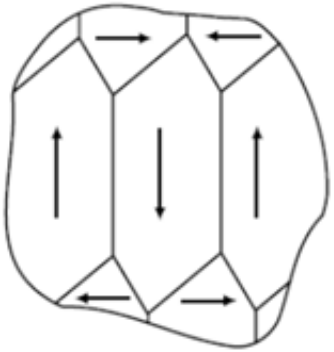

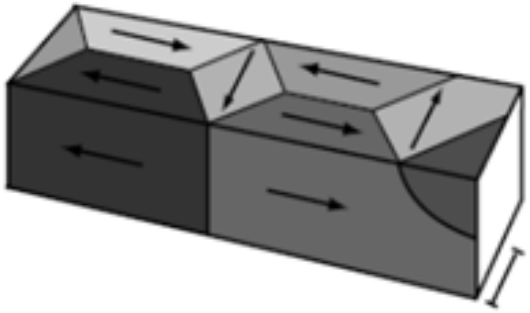

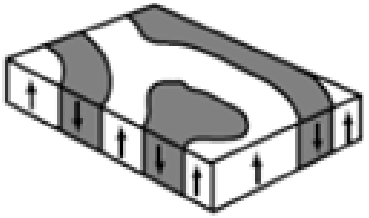

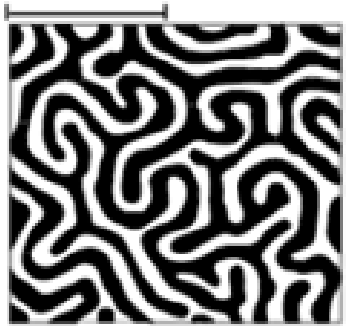

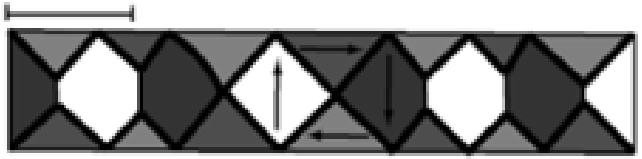

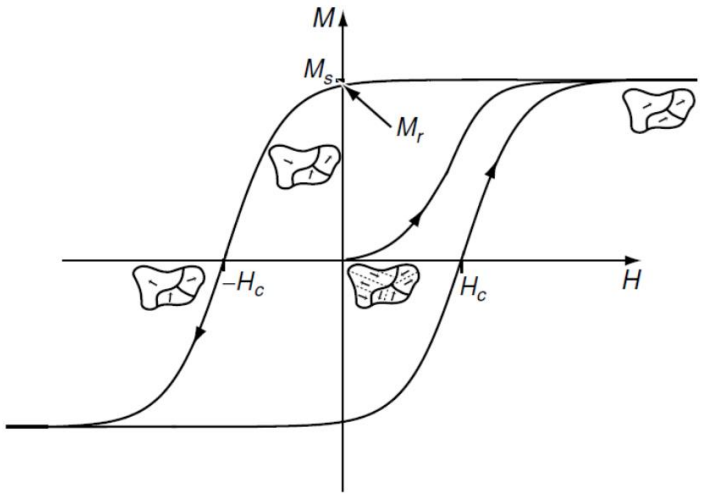

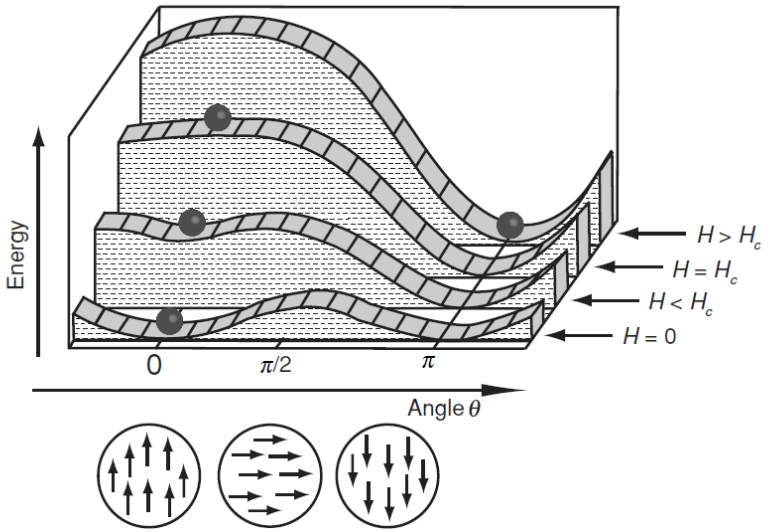

Coercivity and hysteresis are related to a multivalley energy landscape in magnetic configuration space, which exists even for a uniformly magnetized single-domain particle.
There are energy barriers between different magnetization configurations M(r) and jumps from one configuration to another, driven by the external field, are ireversible.

The magnetization reversal process in real materials is **horribly complicated**, generally involving coherent and incoherent reversal processes, as well as nucleation of reverse domains and movement of domain walls.

coherent process
one where the direction of M remains everywhere the same during reversal, independent of r.

incoherent reversal process
an intermediate state which is not uniformly magnetized.

In all but the very smallest, nanometer-sized particles, the reversal process is either incoherent, or it involves an intermediate, multidomain state.

Early progress in understanding coercivity largely relied on simplified models and phenomenological explanations.

More recently largescale computer simulations with software like OOMMF are providing direct insight into the complexity of magnetization reversal.

7.1 Micromagnetic energy

The domain structure is a result of minimizing the total free energy, and it reflects either a local or an absolute energy minimum. There are five other terms besides εd that may have to be considered:

$$\varepsilon_{tot} = \varepsilon_{ex} + \varepsilon_a + \varepsilon_d + \varepsilon_Z + \varepsilon_{stress} + \varepsilon_{ms}.$$

The first three terms due to exchange, magnetocrystalline anisotropy and the demagnetizing field are always present to some extent in a ferromagnet. The fourth is the response to an applied field, and it defines the magnetization process and hysteresis loop. The last terms are due to applied stress and magnetostriction.
We neglect them at first, because the associated energies are small (Table 5.10).

$$\varepsilon_{tot} = \int \{A(\nabla \boldsymbol{M}/M_s)^2 - K_1 \sin^2\theta - \cdots - \tfrac{1}{2}\mu_0 \boldsymbol{M} \cdot \boldsymbol{H}_d - \mu_0 \boldsymbol{M} \cdot \boldsymbol{H}\} \mathrm{d}^3 r.$$

$$(\nabla \boldsymbol{M}/M_s)^2 = (\nabla M_x/M_s)^2 + (\nabla M_y/M_s)^2 + (\nabla M_z/M_s)^2$$

Ms is supposed to remain constant everywhere.
The reference z axis is generally taken as the anisotropy axis.

7.1.1 Exchange

the exchange energy in the continuum picture

$$\varepsilon_{ex} = \int A(\nabla \mathbf{e}_M)^2 \mathrm{d}^3 r,$$

$\mathbf{e}_M = \boldsymbol{M}(\boldsymbol{r})/M_s$

a unit vector in the local direction of magnetization (θ,φ) relative to the z axis

$$\mathbf{e}_M = (\sin\theta\cos\phi, \sin\theta\sin\phi, \cos\theta)$$

$$\varepsilon_{ex} = \int A[(\nabla\theta)^2 + \sin^2\theta(\nabla\phi)^2]\mathrm{d}^3 r.$$

The exchange stiffness A is related to the Curie temperature T_C: A is roughly

$$A \approx k_B T_C/2a_0 \approx \mathcal{J} S^2 Z_c/a_0,$$

a_0 is the lattice parameter

$\mathcal{J}$ the exchange constant

Z_c is the number of atoms per unit cell

7.1.1 Exchange

However, the best way to derive A is from the spin-wave stiffness Dsw in the low-energy magnon dispersion relation (5.56), since the energy of the long-wavelength spinwaves is associated with a gradual twist of the magnetization. The relation is

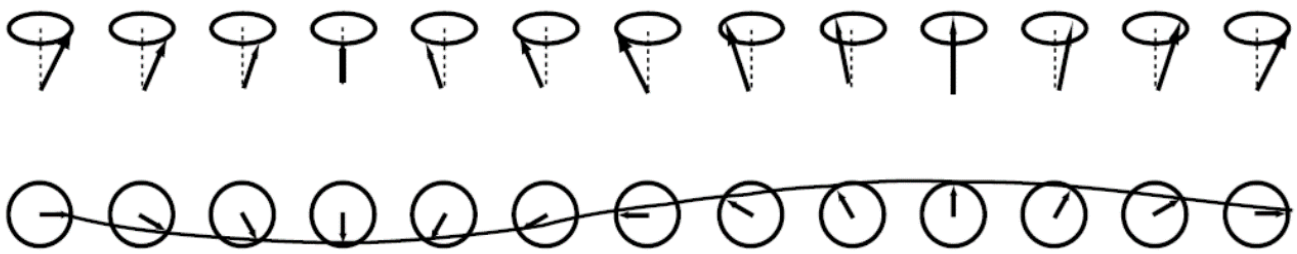

$$\varepsilon_q \approx D_{sw} q^2, \qquad D_{sw} = 2\mathcal{J} S a^2$$

$$A(T) = \frac{M_s(T) D_{sw}}{2 g \mu_B}.$$

7.1.1 Exchange

The competition between the exchange energy εex and the dipolar energy εd is characterized by the exchange length

$$l_{ex} = \sqrt{\frac{A}{\mu_0 M_s^2}}.$$

Other definitions of exchange length can be found in the literature, such as

$$\sqrt{2A/\mu_0 M_s^2}$$

$$\sqrt{A/K_{eff}},$$

K_{eff} : an effective anisotropy constant.

This is the shortest scale on which the magnetization can be twisted in order to minimize the dipolar interaction.

Table 7.1. Domain wall parameters for some ferromagnetic materials

	M_s (MA m^{-1})	A (pJ m^{-1})	K_1 (kJ m^{-3})	δ_w (nm)	γ_w (mJ m^{-2})	κ	l_{ex} (nm)
$Ni_{80}Fe_{20}$	0.84	10	0.15	2000	0.01	0.01	3.4
Fe	1.71	21	48	64	4.1	0.12	2.4
Co	1.44	31	410	24	14.3	0.45	3.4
CoPt	0.81	10	4900	4.5	28.0	2.47	3.5
$Nd_2Fe_{14}B$	1.28	8	4900	3.9	25	1.54	1.9
$SmCo_5$	0.86	12	17 200	2.6	57.5	4.30	3.6
CrO_2	0.39	4	25	44.4	1.1	0.36	4.4
Fe_3O_4	0.48	7	−13	72.8	1.2	0.21	4.9
$BaFe_{12}O_{19}$	0.38	6	330	13.6	5.6	1.35	5.8

7.1.1 Exchange

Stable ferromagnetic configurations in a soft spheroidal particle:
(a) without and (b) with the effect of the demagnetizing field.

Soft magnetic particles with negligible anisotropy tend to adopt a curling or vortex state when they are larger than a certain size, known as the coherence radius.

Magnetic vortex

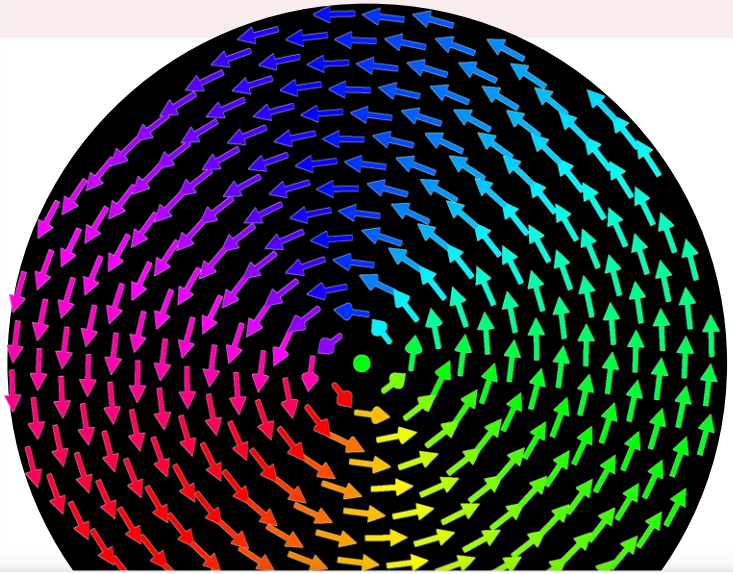

Soft magnetic nanoelement

Fe, Co, Ni, Py ($Fe_{20}Ni_{80}$)

Thickness: 5 ~ 200 nm

Diameter: 50 ~ 2000 nm

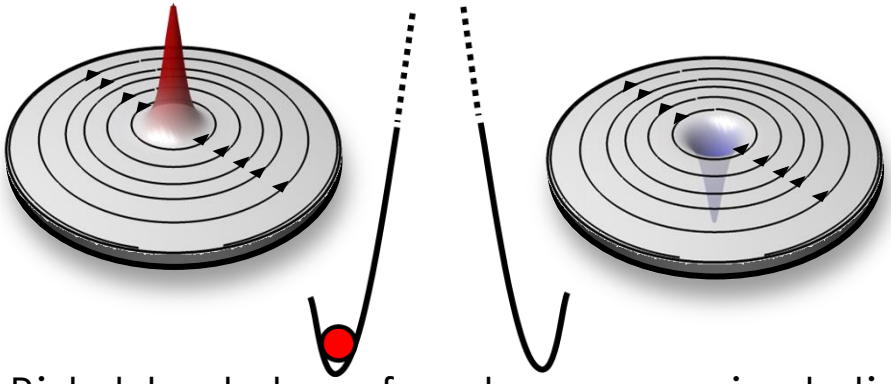

Bistable states of vortex core orientation with high thermal stability

Out-of-plane M at the core (~ 10nm)

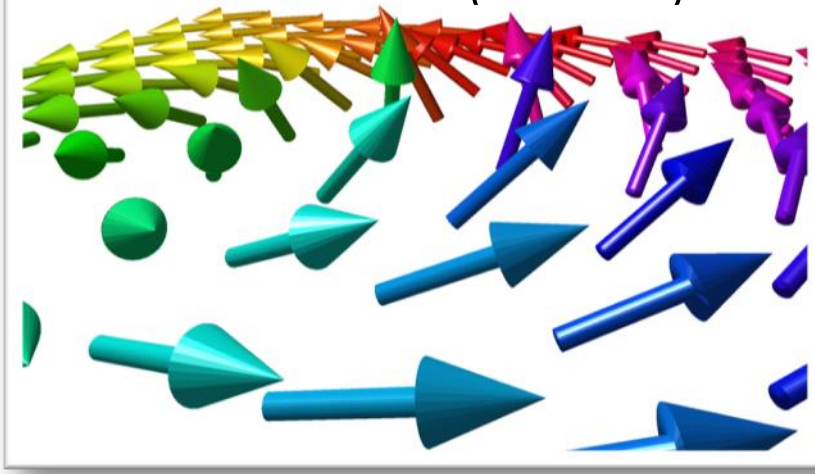

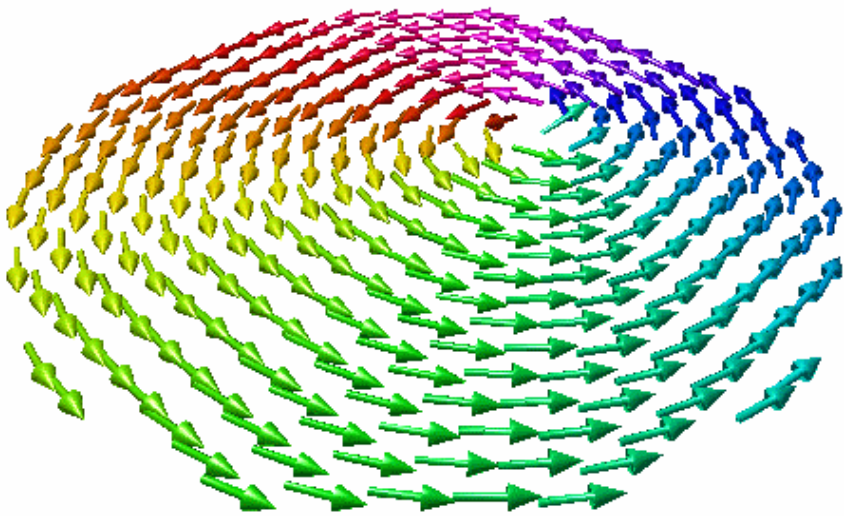

[ν= 1600MHz A= 500Oe] time=0 ps

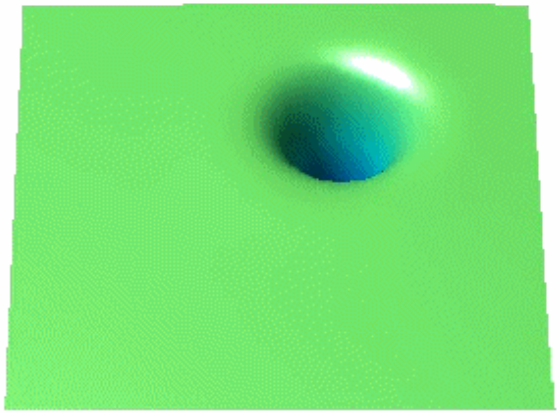

7.1.2 Anisotropy

The anisotropy energy Ea is the single-ion or two-ion magnetocrystalline anisotropy, the leading term of which is

$$K_1 \sin^2 \theta$$

K_1 ranging from 0.1 to 10^4 kJ m^{-3}

Shape anisotropy which is related to the demagnetizing field is included in ε_d .

In each crystallite there are easy directions $\mathbf{e}_n$, which will vary with position in a polycrystalline sample.

The balance of exchange and anisotropy usually leads to a structure in domains where the magnetization lies along an easy axis, separated by narrow domain walls, where the magnetization rotates from one easy direction to another.

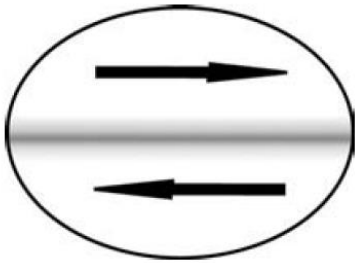

7.1.2 Anisotropy

For thin films and nanoparticles, we have to take into account an additional surface anisotropy term

$$\varepsilon_{as} = \int K_s[1 - (\mathbf{e}_M \cdot \mathbf{e}_n)^2]\mathrm{d}^2 r,$$

$\mathbf{e}_n$ is the surface normal,

the integral is over the sample surface.

K_s are 0.1– 1 mJ m^{-2}.

$$K_{sh} = \tfrac{1}{4}\mu_0 M_s^2(1 - 3\mathcal{N}).$$

order of magnitude of shape anisotropy for a ferromagnet with $\mu_0 M_s \approx 1$ T

200 kJ m^{-3} when $\mathcal{N} = 0$.

7.1.2 Anisotropy

Exchange-related anisotropy may be present when there is coupling at a ferromagnetic–antiferromagnetic or soft–hard interface.
Unlike the other forms of anisotropy, this one is unidirectional,

$$\varepsilon_{ea} = -\int K_{ex} \cos\theta \, \mathrm{d}^2 r,$$

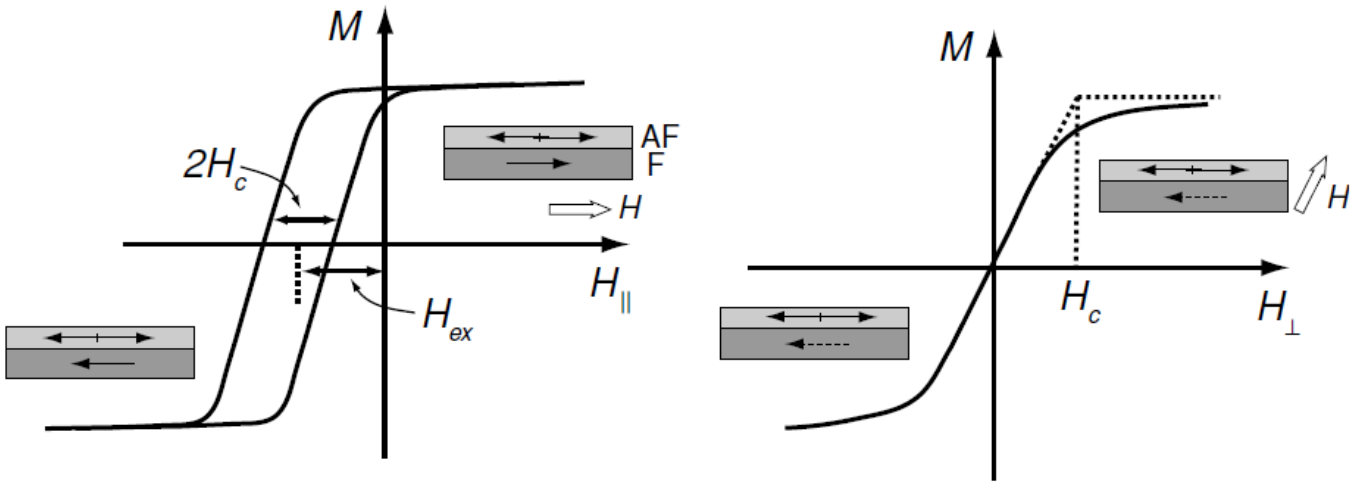

7.1.3 Demagnetizing field

When no external field is present, it follows from

$$\boldsymbol{B} = \mu_0(\boldsymbol{H} + \boldsymbol{M})$$

$$\nabla \cdot \boldsymbol{B} = 0$$

$$\nabla \cdot \boldsymbol{H}_d = -\nabla \cdot \boldsymbol{M}.$$

$$\int \boldsymbol{B} \cdot \boldsymbol{H} \mathrm{d}^3 r = 0,$$

where the integral is over all space, it follows that the demagnetizing energy (7.1) can be written in two equivalent ways:

$$\varepsilon_d = -\tfrac{1}{2} \int \mu_0 \boldsymbol{H}_d \cdot \boldsymbol{M} \mathrm{d}^3 r \qquad \text{(integral over the volume of the magnet)} \tag{7.9}$$

$$\varepsilon_d = \tfrac{1}{2} \int \mu_0 H_d^2 \mathrm{d}^3 r \qquad \text{(integral over all space).}$$

Values of E_d range up to 2000 kJ m^{-3}.

7.1.6 Charge avoidance

The task of understanding how nature minimizes the sum of all six terms in the micromagnetic free energy of a ferromagnetic specimen to arrive at a stable configuration is a formidable one. Vortex states tend to be stable in soft ferromagnets, multidomain states in hard ferromagnets and single-domain states in the smallest ferromagnetic elements.
A rough but useful guide for minimizing the energy in a multidomain body is **the charge avoidance principle.**

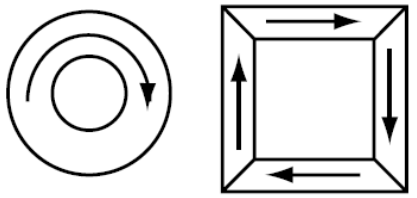

- Surface charge $\mathbf{M} \cdot \mathbf{e}_n$ is loathe to form, because of the high energy cost of the stray field $\mathbf{H}_d$ which it creates (2.79).
- Charges of the same sign tend to avoid each other as far as possible for the same reason.
- The magnetization in the bulk should have as little divergence as possible to avoid creating volume charge $\nabla \cdot \mathbf{M}$.

Complete freedom of the magnetization to rotate in order to maximize charge avoidance implies an absence of anisotropy that is characteristic of very soft magnetic material.

7.1.6 Charge avoidance

An elegant construction due to van den Berg produces 'pole-free' configurations in thin-film elements that depend only on the shape of the element.

His method ensures that

- The magnetization is everywhere parallel to the surface.
- The domain walls are the locus of points corresponding to the centre of a circle which touches the edge of the element at two points at least, but does not cut it anywhere.
- The magnetization pattern so obtained is not only parallel to the surface, but also divergenceless in the interior.
- Walls end at singular points within the element, or else at sharp corners.
- Virtual cuts can be introduced anywhere in the element to create new domains,

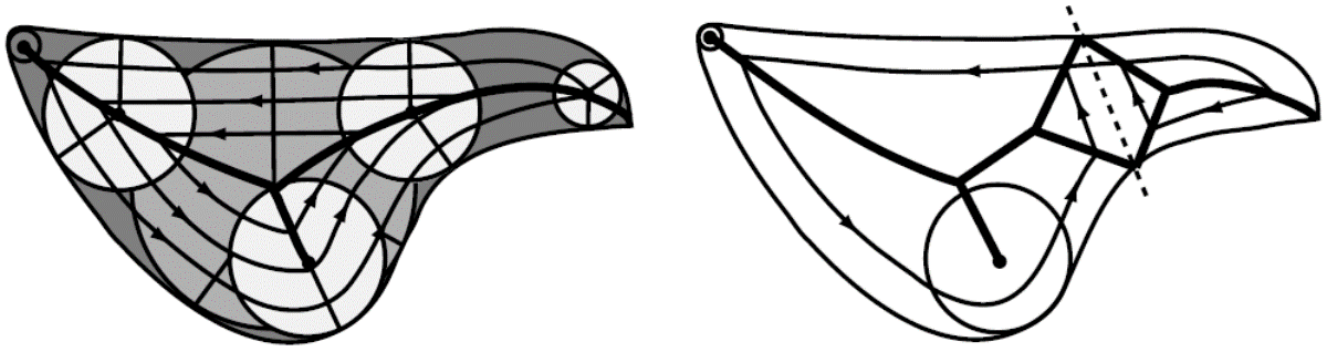

7.1.6 Charge avoidance

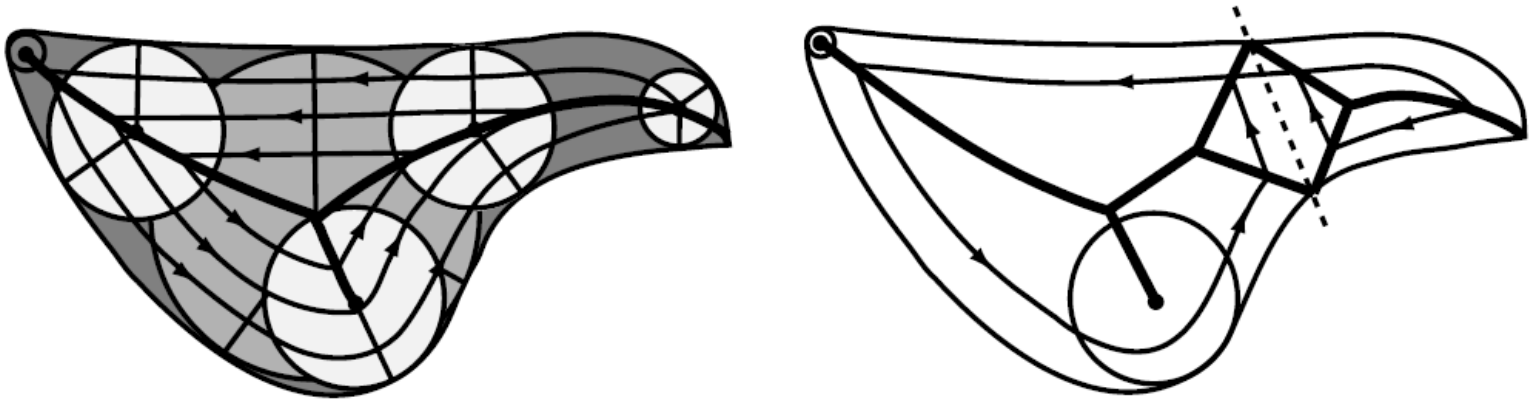

The cost in exchange energy of forming the domain walls needed to achieve the ‘pole-free’ configurations is overlooked, but charge avoidance provides us with an idea of the magnetic configurations which would arise from the influence of dipole interactions alone.
It is best applied to soft magnetic films with little anisotropy and dimensions which exceed the domain wall width.

A permanent magnet is the antithesis of charge avoidance. Here the purpose is to generate as much stray field as possible in surrounding space. Permanent magnets are characterized by lots of surface charge and deep metastable minima in their energy landscape which make configurations with close-to-saturated magnetization stable almost indefinitely. The anisotropy term in (7.5) is the key to achieving this.

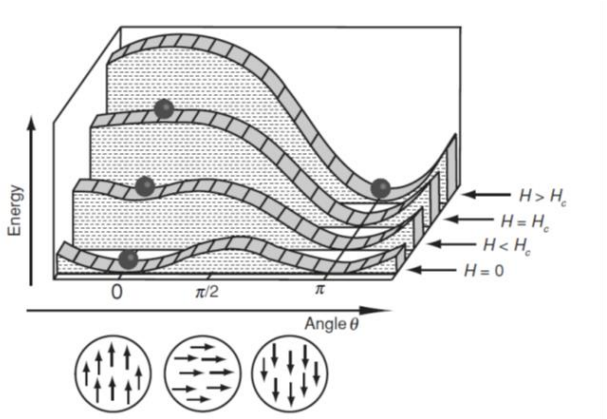

Brown's micromagnetic equations

$$\varepsilon_{tot} = \varepsilon_{ex} + \varepsilon_a + \varepsilon_d + \varepsilon_Z + \varepsilon_{stress} + \varepsilon_{ms}. \qquad (7.4)$$

$$\varepsilon_{tot} = \int \{A(\nabla \boldsymbol{M}/M_s)^2 - K_1 \sin^2\theta - \cdots - \tfrac{1}{2}\mu_0 \boldsymbol{M}\cdot\boldsymbol{H}_d - \mu_0 \boldsymbol{M}\cdot\boldsymbol{H}\}\mathrm{d}^3 r. \qquad (7.5)$$

Generally, the minimization of (7.4) or (7.5) involves finding a solution where the magnetization direction is stable at every point, subject to boundary conditions.
If $\boldsymbol{H}_{eff}$ is the local effective field, which makes an angle ϑ with the local magnetization direction $\mathbf{e}_M$, the condition

$$\partial E_{tot}/\partial\vartheta = 0$$

means that

$$-M H_{eff} \sin\vartheta = 0$$

This is equivalent to the condition that no torque acts anywhere on the magnetization;

$$\boldsymbol{\Gamma} = \boldsymbol{M} \times \boldsymbol{H}_{eff} = 0$$

$$\mathbf{e}_M \times \boldsymbol{H}_{eff} = 0.$$

Brown's micromagnetic equations

$$\varepsilon_{tot} = \int \{A(\nabla \boldsymbol{M}/M_s)^2 - K_1 \sin^2\theta - \cdots - \tfrac{1}{2}\mu_0 \boldsymbol{M}\cdot\boldsymbol{H}_d - \mu_0 \boldsymbol{M}\cdot\boldsymbol{H}\}\mathrm{d}^3 r. \tag{7.5}$$

$$\boldsymbol{H}_{eff} = \frac{2A}{\mu_0 M_s}\nabla^2 \mathbf{e}_M - \frac{1}{\mu_0 M_s}\frac{\partial E_a}{\partial \mathbf{e}_M} + H_d + H'. \tag{7.13}$$

$$\nabla^2 \mathbf{e}_M = M_s^{-1}[(\partial^2 M_x/\partial x^2 + \partial^2 M_x/\partial y^2 + \partial^2 M_x/\partial z^2), \ldots],$$

$$\partial E_a/\partial \mathbf{e}_M = [\partial E_a/\partial \mathbf{e}_{Mx}, \partial E_a/\partial \mathbf{e}_{My}, \partial E_a/\partial \mathbf{e}_{Mz}]$$

These two are Brown's micromagnetic equations, which have to be solved numerically, subject to the surface boundary condition

$$\mathbf{e}_M \times \left[2A(\mathbf{e}_n \cdot \nabla)\mathbf{e}_M + \frac{\partial E_{as}}{\partial \mathbf{e}_M}\right] = 0.$$

Their meaning is that in equilibrium the magnetization lies everywhere parallel to $\boldsymbol{H}_{eff}$ given by (7.13).

7.2 Domain theory

The micromagnetic approach is capable, ***in principle***, of predicting the equilibrium magnetic configurations of any system where the exchange stiffness $A(r)$ and anisotropy $Ea(r)$ can be specified throughout.

Hysteresis may be deduced, knowing the magnetic history in an applied field $\boldsymbol{H}'(t)$.
No account is taken of temperature.
It is impractical to implement micromagnetic theory in any but idealized situations.

The problem is mathematically complex, and real materials contain local defects and disorder which cannot be specified precisely, but which nonetheless tend to dominate the magnetization process.

Domain theory breaks down in very soft magnetic materials, especially in thin film elements where the demagnetizing field is small. There, instead of domains, states with continuous rotation of magnetization tend to form.

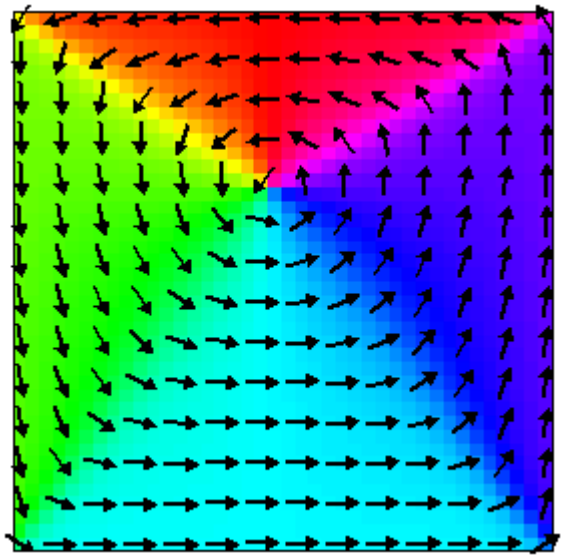

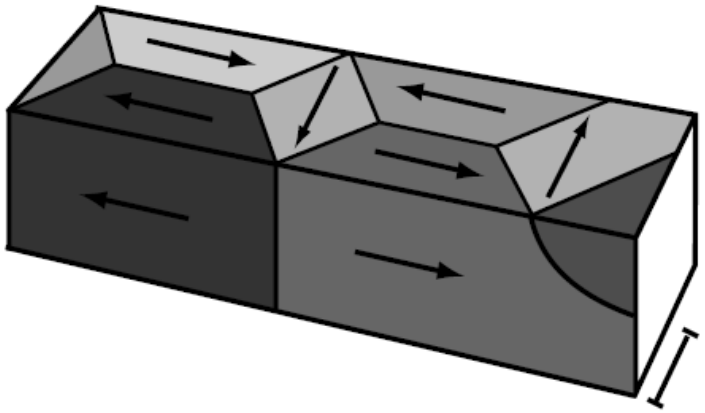

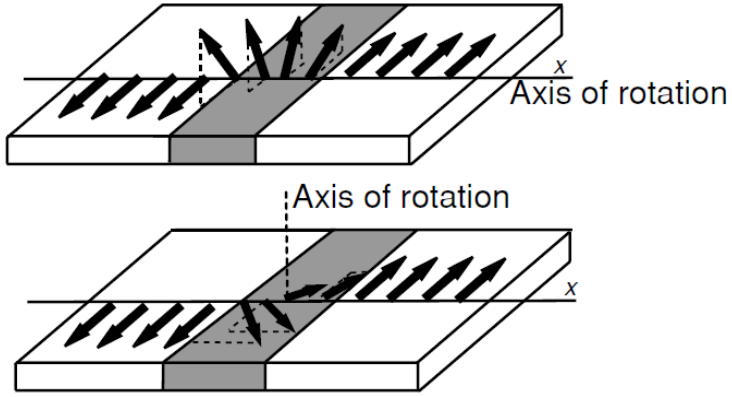
x
Axis of rotation
Axis of rotation
x

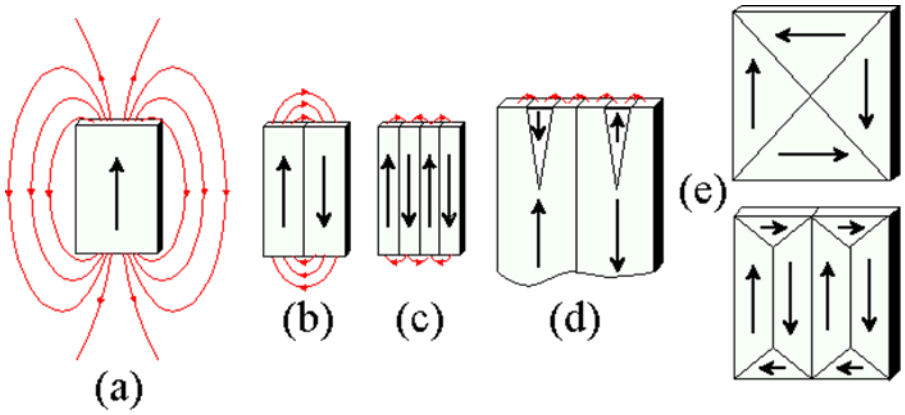
(a)
(b)
(c)
(d)
(e)

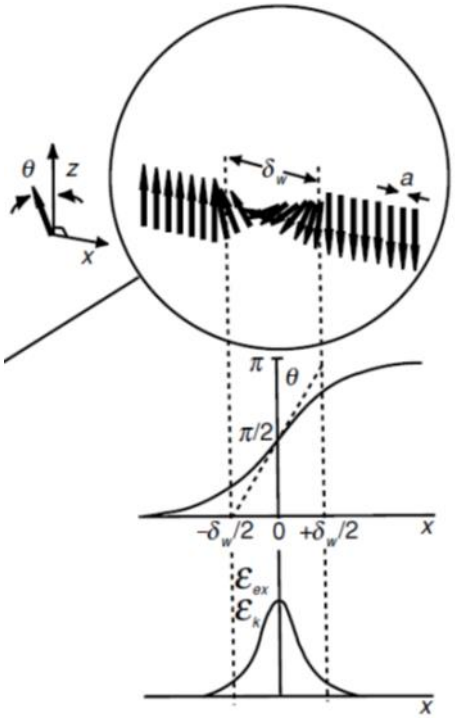
θ
z
x
δw
a
π
θ
π/2
−δw/2
0
+δw/2
x
εex
εk
x

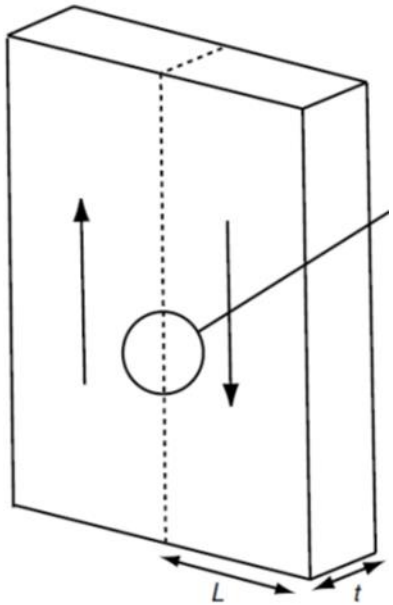
L
t

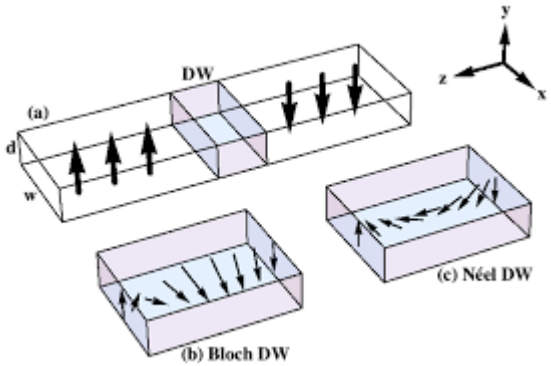
y
z
x
DW
(a)
d
w
(c) Néel DW
(b) Bloch DW

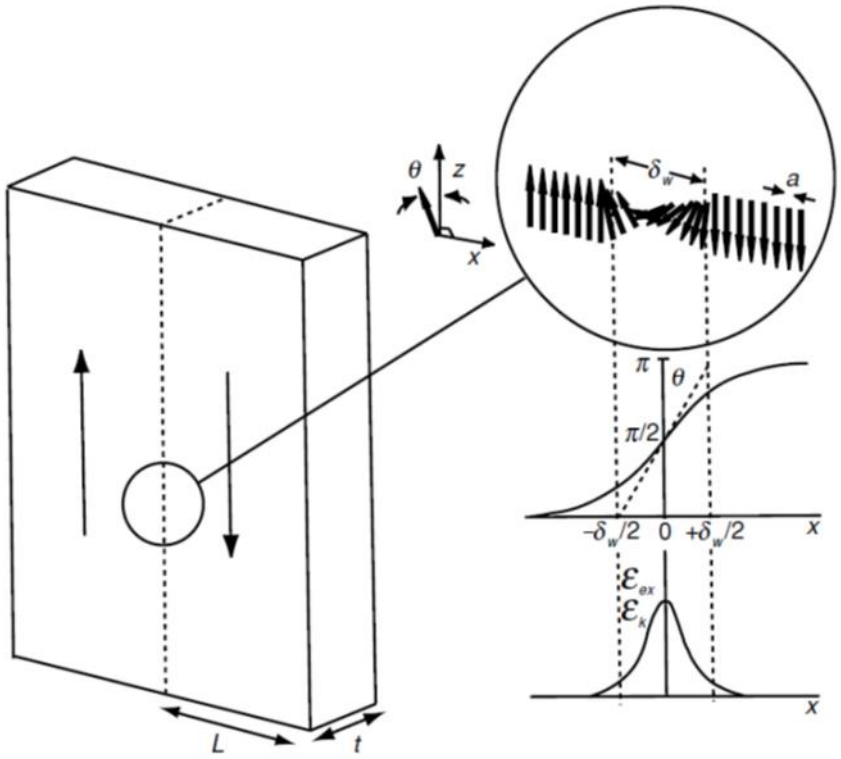

$$\delta_w \approx \sqrt{A/K_1}, \text{ which is of order 10–100 nm,}$$

$$\gamma_w \approx \sqrt{AK_1}, \quad \text{order 1 mJ m}^{-2}$$

$$4\mathcal{J}S^2/a^2 \approx 2A/a \text{ or about } 0.1 \text{ J m}^{-2}$$

7.2.1 Bloch wall

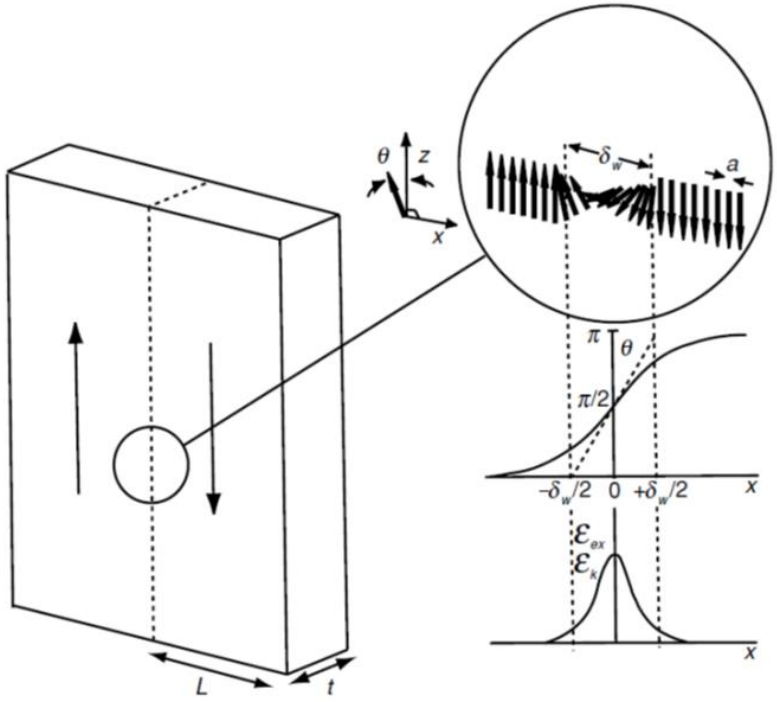

The Bloch wall has the remarkable property that it creates no divergence of the magnetization.

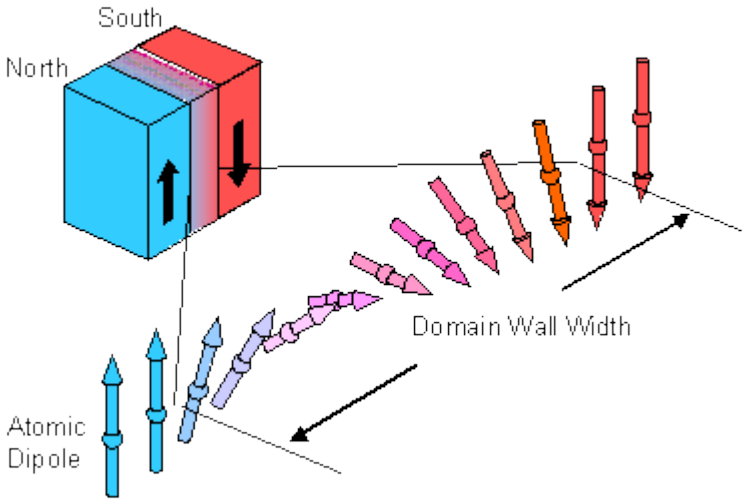

$$\nabla \cdot \boldsymbol{M} = \partial M_x/\partial x + \partial M_y/\partial y + \partial M_z/\partial z \text{ is zero}$$

there is no component of magnetization in the x-direction, and the spins in each yz-plane are parallel to each other.
no magnetic charge and no source of demagnetizing field in the wall.

7.2.1 Bloch wall

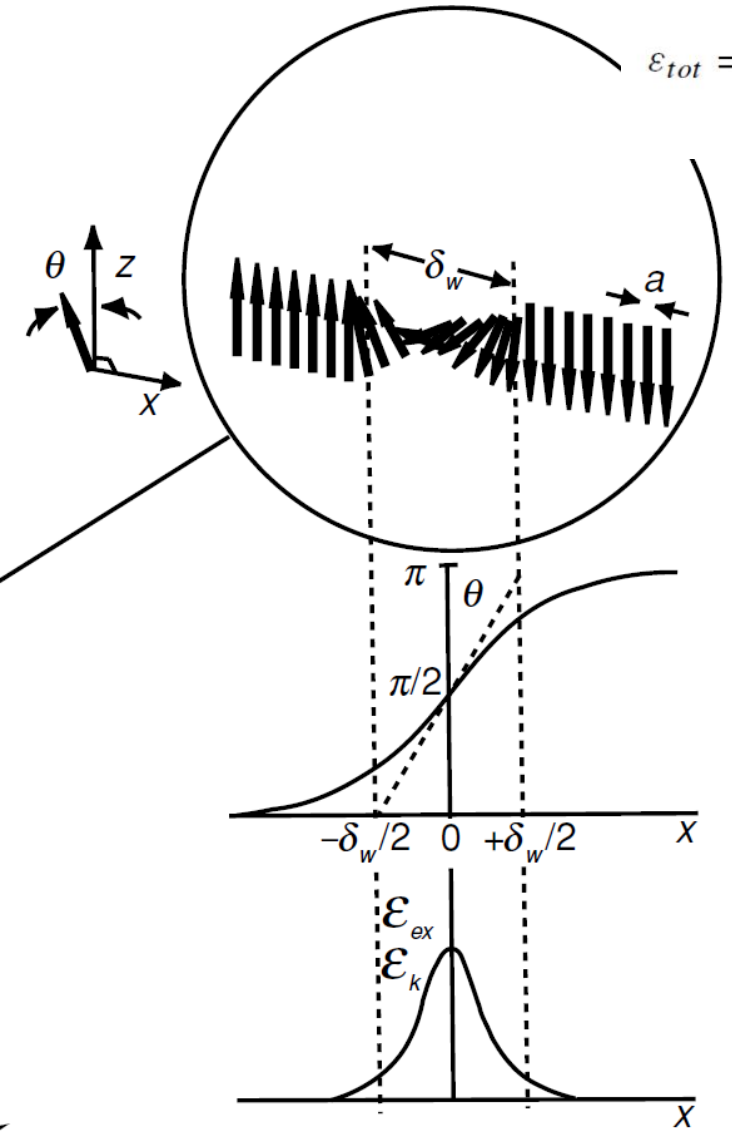

$$\varepsilon_{tot} = \int \{A(\nabla \boldsymbol{M}/M_s)^2 - K_1 \sin^2\theta - \cdots - \tfrac{1}{2}\mu_0 \boldsymbol{M}\cdot\boldsymbol{H}_d - \mu_0 \boldsymbol{M}\cdot\boldsymbol{H}\}\mathrm{d}^3 r. \tag{7.5}$$

To calculate the form of the Bloch wall, we minimize the free energy (7.5) for clockwise (or anticlockwise) rotation. Ignoring the magnetostatic energy originating at the sample surface, and considering only the leading anisotropy term

$$\varepsilon_{tot} = \varepsilon_{ex} + \varepsilon_k = \int [A(\partial\theta/\partial x)^2 + K\sin^2\theta]\mathrm{d}x.$$

Minimizing the integral, which is of the form

$$\int F(x, \theta(x), \theta'(x))\mathrm{d}x,$$

$$\partial F/\partial\theta - (\mathrm{d}/\mathrm{d}x)(\partial F/\partial\theta') = 0 \qquad \theta' = \partial\theta/\partial x$$

$$\partial(K\sin^2\theta)/\partial\theta - 2A\partial^2\theta/\partial x^2 = 0.$$

7.2.1 Bloch wall

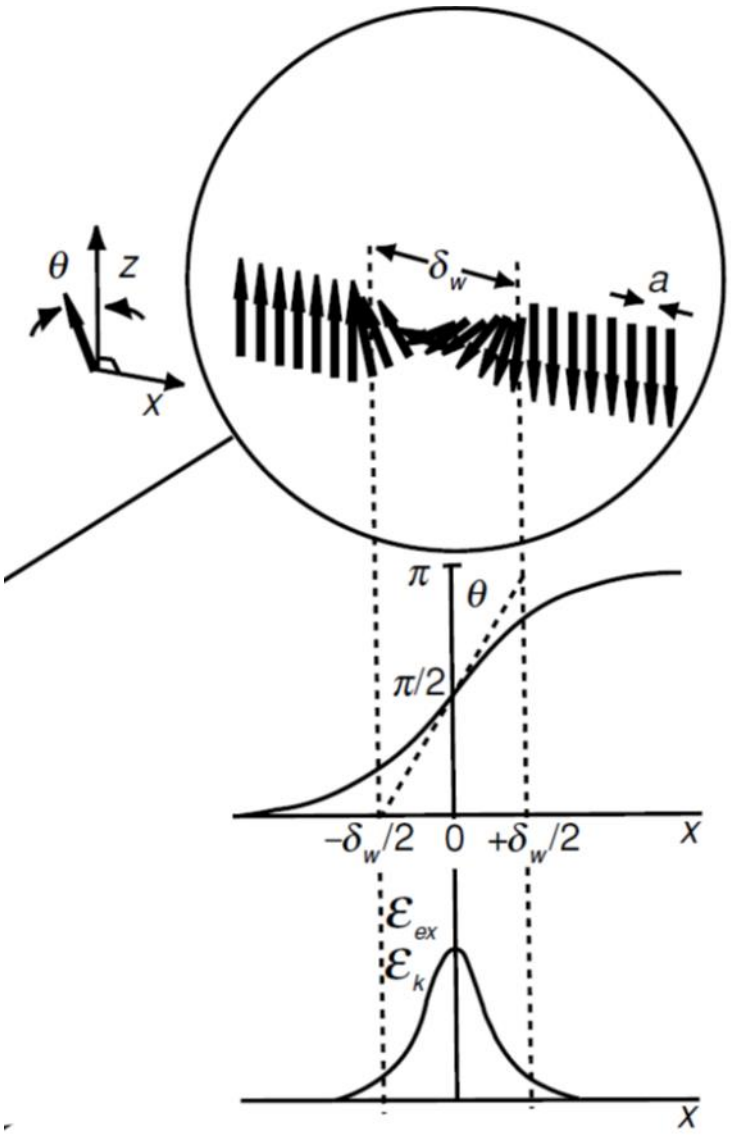

$$\partial(K \sin^2\theta)/\partial\theta - 2A\partial^2\theta/\partial x^2 = 0.$$

$$K \sin^2\theta = A(\partial\theta/\partial x)^2$$

$$\partial\theta/\partial x = \sqrt{K/A}\sin\theta$$

$$x = \sqrt{\frac{A}{K}}\ln\tan(\theta/2),$$

where $\theta = \pi/2$ at the origin,

$$\theta(x) = \tan^{-1}[\sin k(\pi x/\delta_w)] + \pi/2,$$

$$\delta_w = \pi\sqrt{\frac{A}{K}}.$$

7.2.1 Bloch wall

The domain wall does not have a precisely defined width, since the direction of magnetization only approaches 0 or π asymptotically.

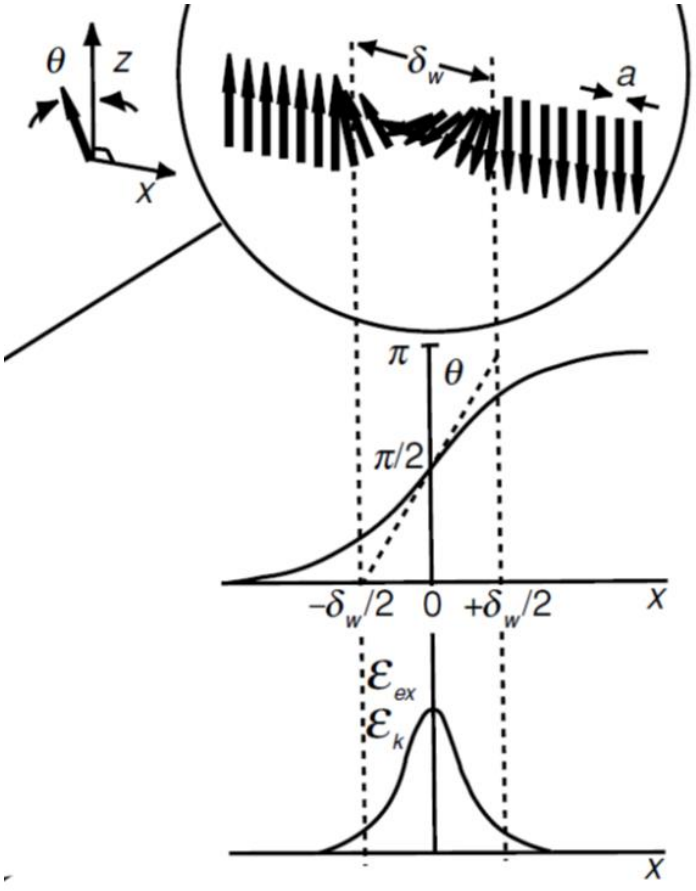

the extrapolated width from the tangent at the origin

the width as the distance between points where some fraction, say 90%, of the rotation has taken place.

$$\delta_w \approx 4\sqrt{(A/K)}$$

$$K \sin^2\theta = A(\partial\theta/\partial x)^2$$

the two terms in the integral (7.14) for the energy are equal to each other at every point in the wall.

The energy per unit domain wall area is

$$\gamma_w = 4\sqrt{AK}.$$

7.2.1 Bloch wall

Table 7.1. Domain wall parameters for some ferromagnetic materials

	M_s (MA m^{-1})	A (pJ m^{-1})	K_1 (kJ m^{-3})	δ_w (nm)	γ_w (mJ m^{-2})	κ	l_{ex} (nm)
$Ni_{80}Fe_{20}$	0.84	10	0.15	2000	0.01	0.01	3.4
Fe	1.71	21	48	64	4.1	0.12	2.4
Co	1.44	31	410	24	14.3	0.45	3.4
CoPt	0.81	10	4900	4.5	28.0	2.47	3.5
$Nd_2Fe_{14}B$	1.28	8	4900	3.9	25	1.54	1.9
$SmCo_5$	0.86	12	17 200	2.6	57.5	4.30	3.6
CrO_2	0.39	4	25	44.4	1.1	0.36	4.4
Fe_3O_4	0.48	7	−13	72.8	1.2	0.21	4.9
$BaFe_{12}O_{19}$	0.38	6	330	13.6	5.6	1.35	5.8

7.2.2 Néel wall

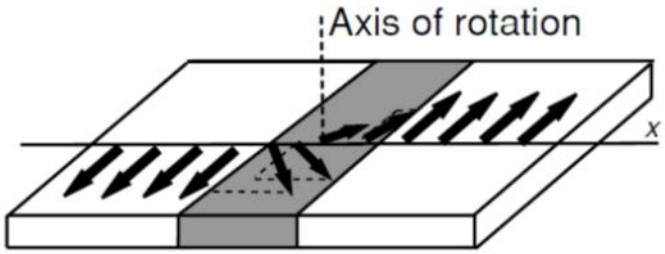

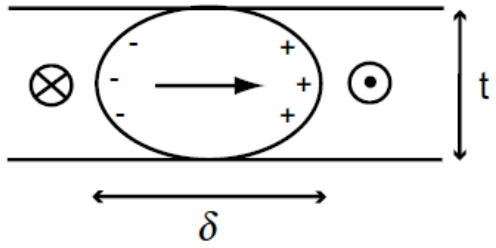

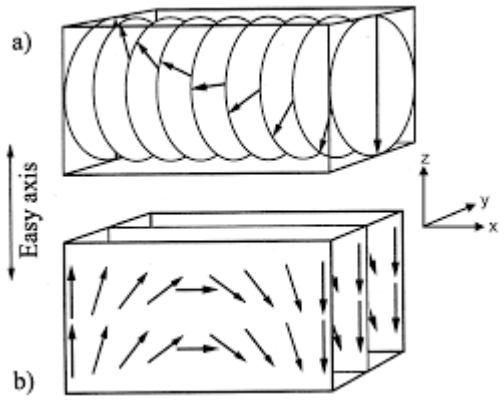

The Néel wall, where the magnetization rotates within the plane of the domain magnetization, is normally higher in energy than the Bloch wall because of the stray field created by the nonzero divergence of M.

Domain walls in thin films

the Bloch wall -> surface charge

the Néel wall creates no surface charge, and there is no associated stray field.

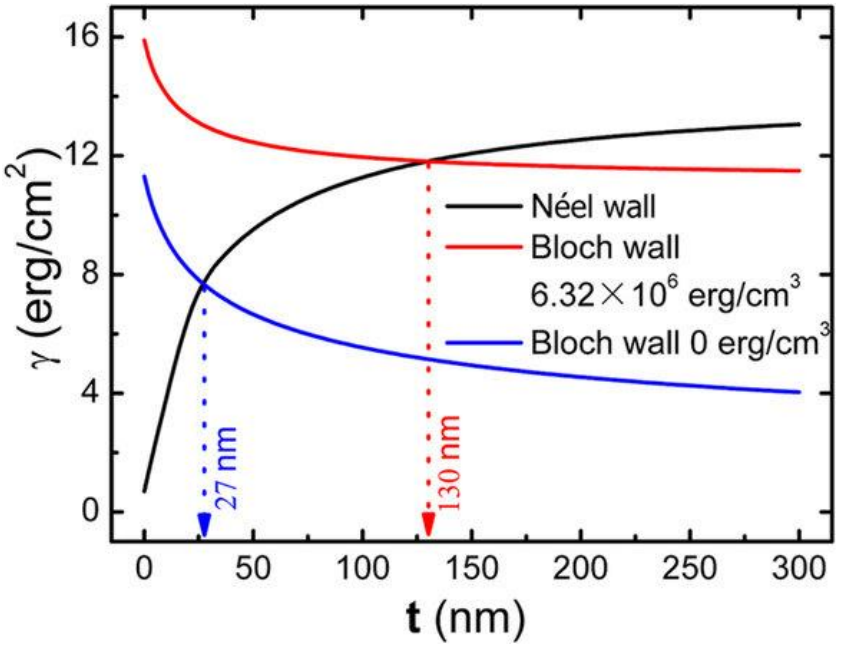

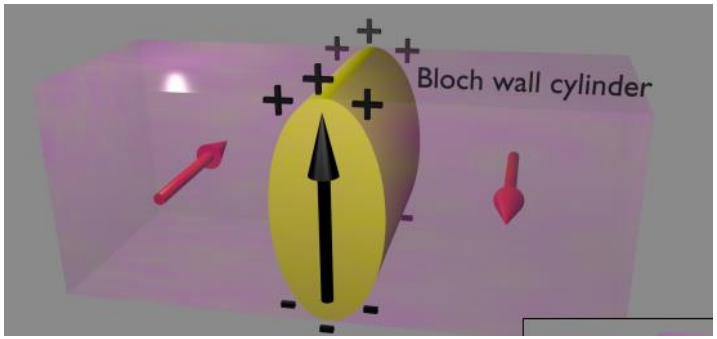

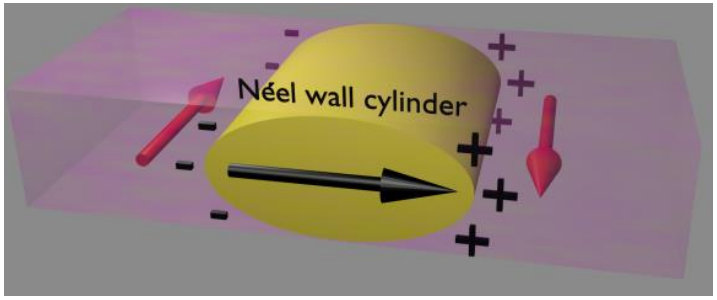

Domain walls in thin films

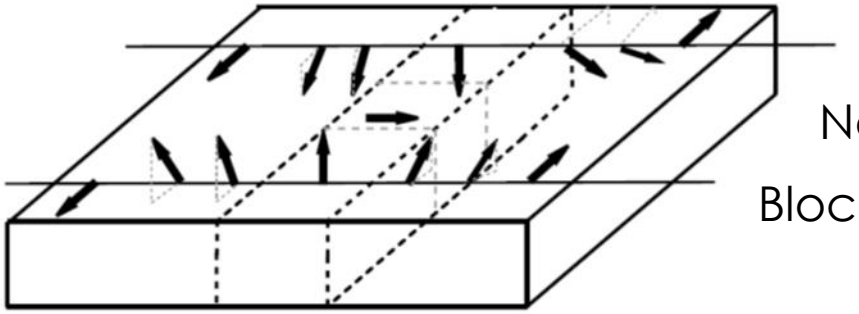

Bloch wall

Neel line (Bloch line)

Bloch wall

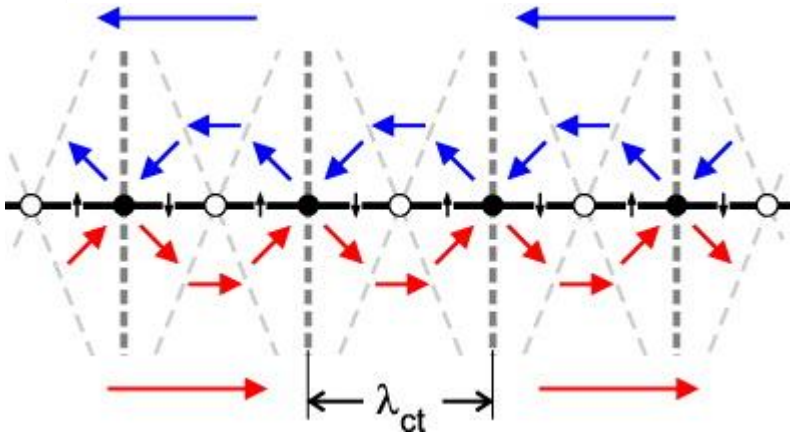

A cross-tie wall is a N´eel wall in which the magnetization rotates in opposite directions in adjacent sections. Transitions between domains in thicker films may have vortex structures, mixtures with N´eel caps at the surface and Bloch character at the centre. There is rich fauna in the micromagnetic jungle.

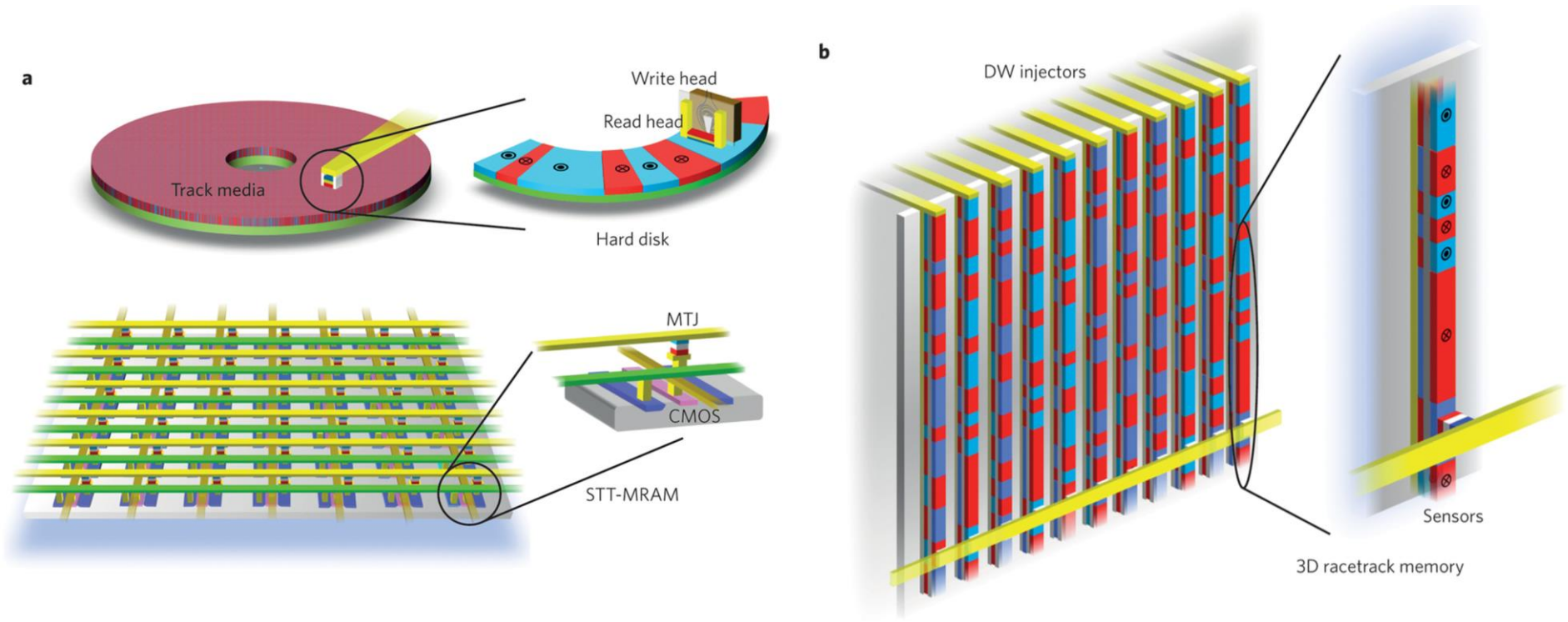
a
Write head
Read head
Track media
Hard disk
MTJ
CMOS
STT-MRAM
b
DW injectors
Sensors
3D racetrack memory

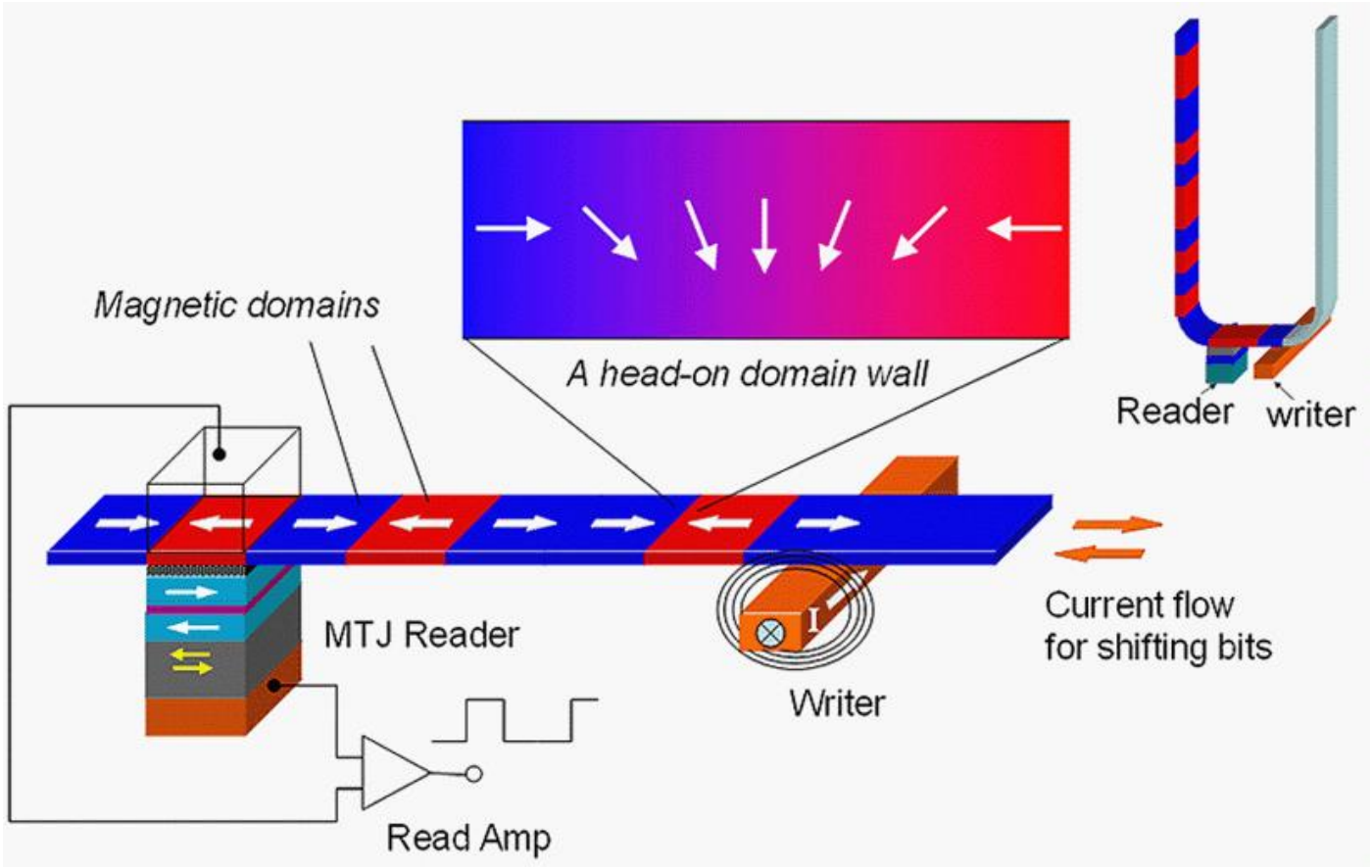
Magnetic domains
A head-on domain wall
Reader
writer
MTJ Reader
Writer
Current flow
for shifting bits
Read Amp

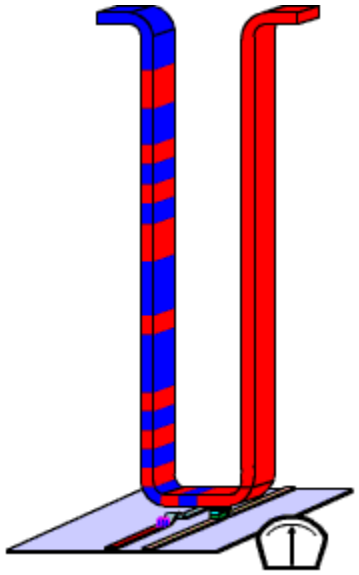

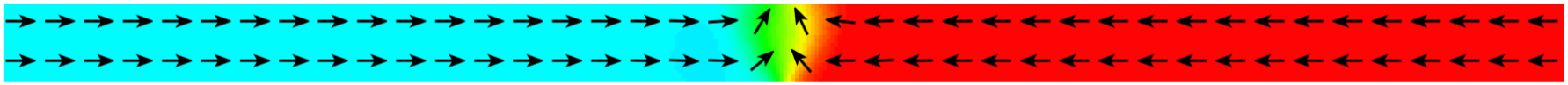

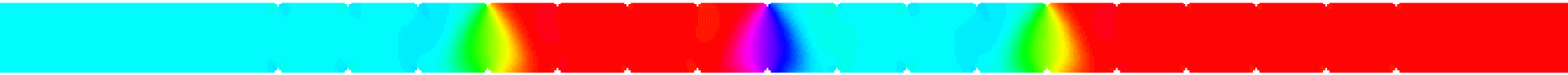

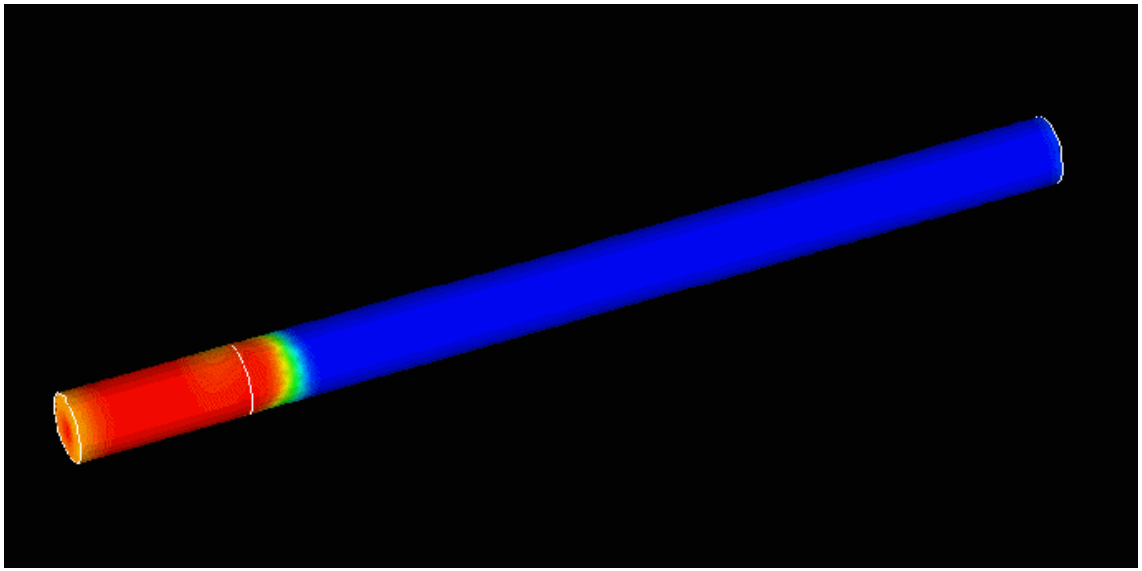

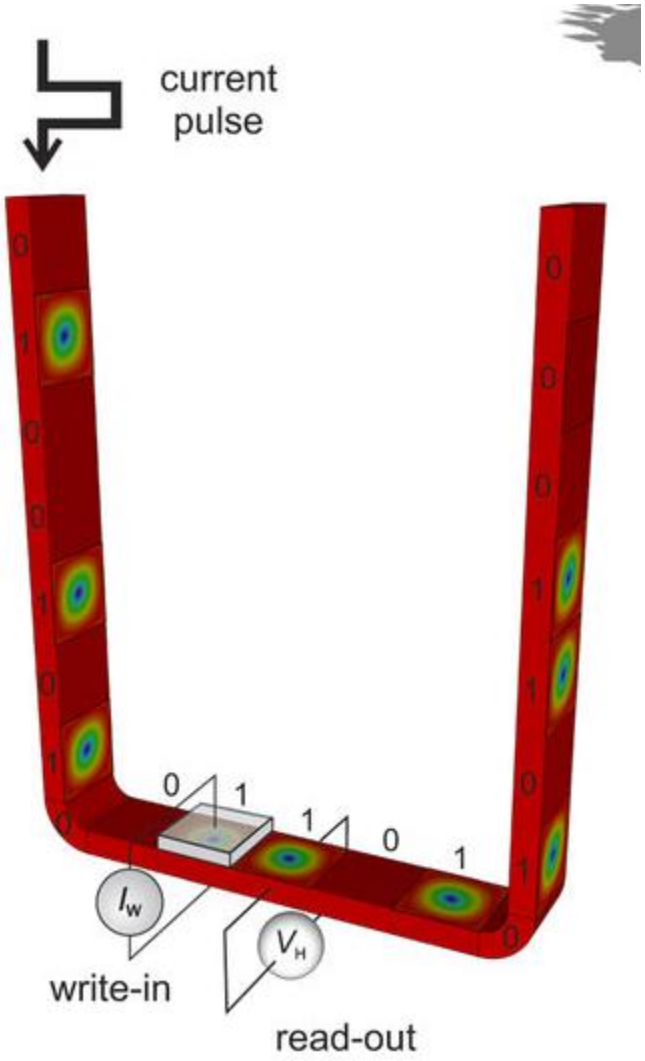
current
pulse
0
1
1
0
1
I_w
write-in
V_H
read-out

7.2.3 Magnetization processes

The domain picture is a good one for ferromagnetic solids, when the domain size is much greater than the domain wall width.

the two basic magnetization processes in any multi domain solid:

- Domain wall motion
- Domain rotation

7.3 Reversal, pinning and nucleation

Hysteresis would never exist unless there was some chance of a ferromagnetic specimen getting stuck in a metastable configuration with a remanant magnetization and higher energy than the absolute minimum energy configuration

In order to make some sense of the complex problem of hysteresis, we first examine the magnetization reversal in a single-domain particle or thin-film element, which can be calculated analytically.

Then we look into how domain theory allows us to formulate the elementary processes involved in coercivity in multidomain samples.

7.3 Reversal, pinning and nucleation

In 1947 William Fuller Brown proved rigorously that the coercivity for a homogeneous, uniformly magnetized ellipsoid obeys the inequality

$$H_c \geq (2K_1/\mu_0 M_s) - \mathcal{N} M_s,$$

a surprising result known in micromagnetics as **Brown's theorem**.

In reality, coercivity in bulk material is never this large.

It is generally a long struggle, following the introduction of a new hard magnetic material, to achieve a coercivity that exceeds 20–30% of the anisotropy field (Fig. 7.8).
This apparent contradiction between theory and practice is known as **Brown's paradox**.

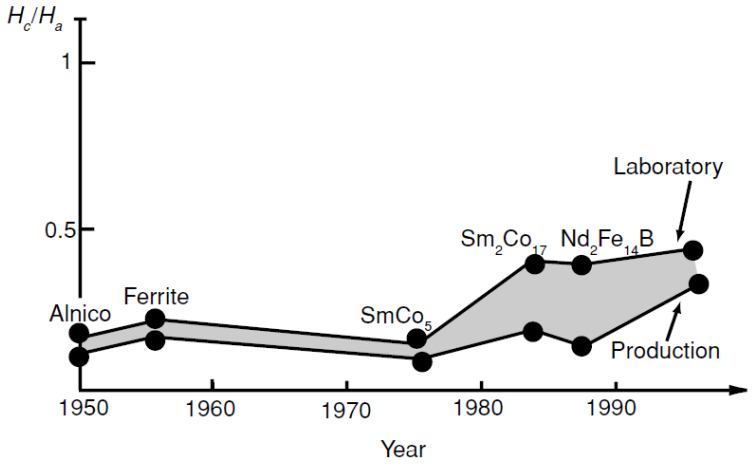

7.3 Reversal, pinning and nucleation

the assumptions of the theory are not met in practice. All real materials are inhomogeneous, and magnetization reversal is initiated in a small nucleation volume around a defect.

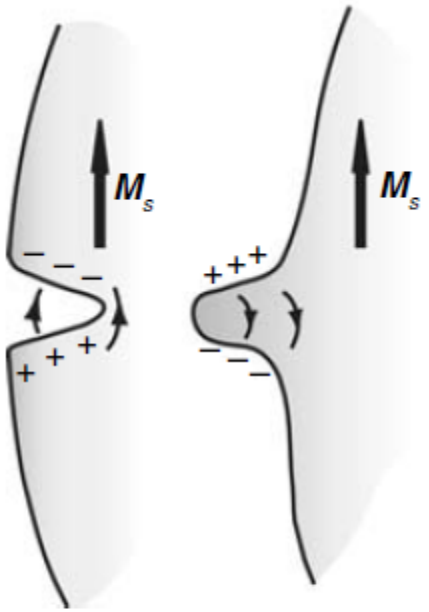

Local stray fields near a surface pit or bump. The region prone to reversal is shaded.

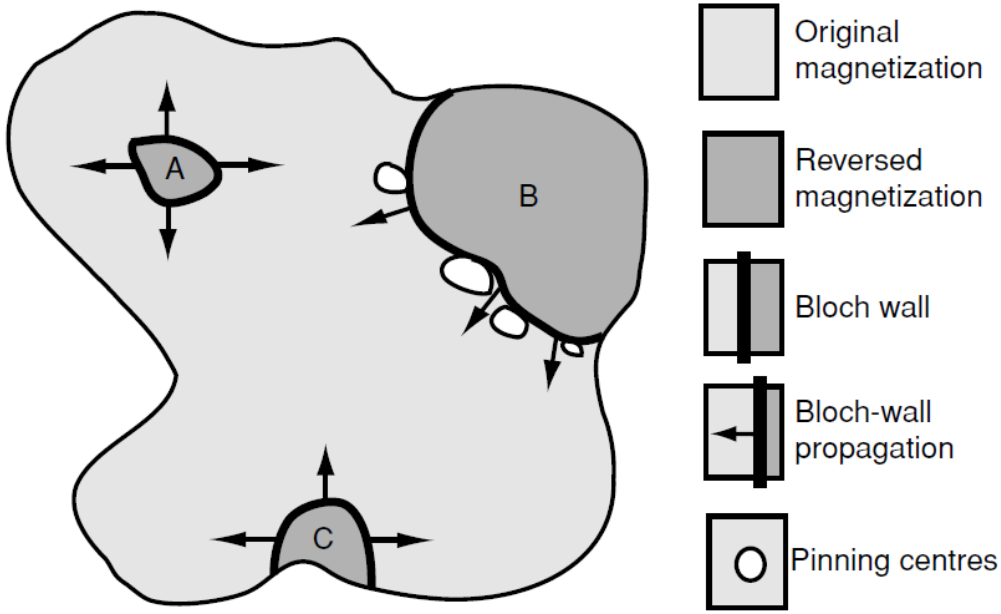

A : reverse domain which nucleates in the bulk at a defect, or from a spontaneous thermal fluctuation.

B : a reverse domain which has grown to the point where it is trapped by pinning centres

C : a reverse domain which nucleates at a surface asperity.

7.3 Reversal, pinning and nucleation

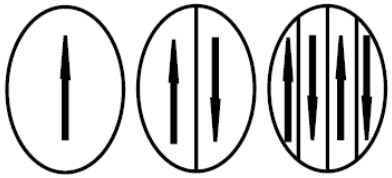

A magnetic particle reduces its energy by forming domains.

Very small magnetic particles must be single-domain; they do not benefit energetically from wall formation if they are below a certain critical size.

Consider a spherical particle of radius R with cubic anisotropy, which forms two 90 domain walls in order to almost eliminate the stray field.

The cost of creating the two walls,

$$2\pi R^2 \sqrt{A K_{1c}},$$

must be offset by the gain in demagnetizing energy of the sphere,

$$-\tfrac{1}{2}\mu_0 \mathcal{N} V M_s^2$$

$$\mathcal{N} = 1/3$$

$$R_{sd} \approx 9\sqrt{A K_{1c}}/\mu_0 M_s^2.$$

7.3 Reversal, pinning and nucleation

Two or three different modes of reversal can occur in a single-domain particle.

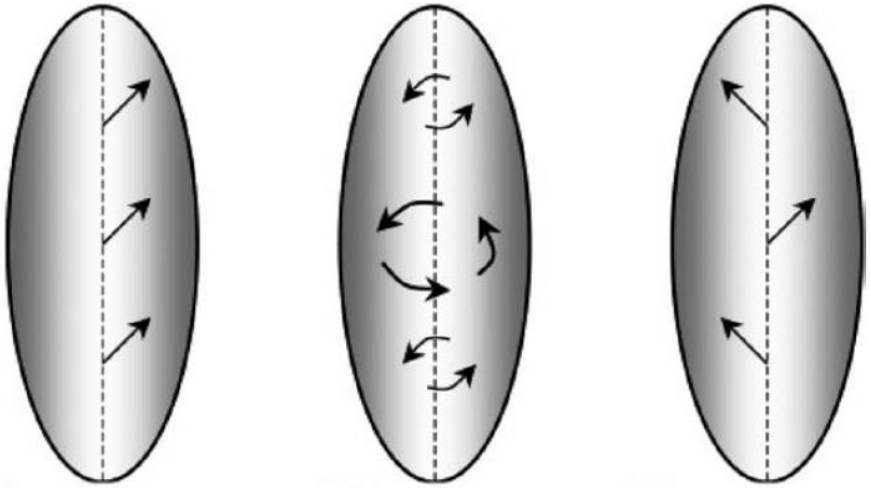

Coherent rotation mode where the magnetization remains uniform Everywhere, and it rotates in unison, increasing the stray field as it flips through A configuration where the magnetization is perpendicular to the easy axis.

Curling mode which avoids creating stray field by passing through a vortex state where the magnetization lies everywhere parallel to the surface This costs exchange energy. The vortex state is the lowest energy state of soft magnetic particles which are larger than the coherence radius.

Buckling which is a combination of the other two that creates less stray field than coherent rotation.

The simplest model of magnetization reversal, the Stoner–Wohlfarth model, assumes the coherent mode of magnetization reveral. The magnetization is supposed to remain uniformas its orientation changes with time during reversal.
However, even if a particle is smaller than Rsd , magnetization reversal does not
have to be coherent. Other possible reversal modes, curling and buckling, are
illustrated in Fig. 7.10. Curling is the one which arises in spherical particles which are larger than the coherence radius.

7.3.1 Stoner–Wohlfarth model

The simplest model of magnetization reversal, the Stoner–Wohlfarth model, assumes the coherent mode of magnetization reversal.
The magnetization is supposed to remain uniformas its orientation changes with time during reversal.

Imagine a Stoner–Wohlfarth particle, a uniformly magnetized ellipsoid with uniaxial anisotropy of shape or magnetocrystalline origin in a field applied at an angle a to the anisotropy axis

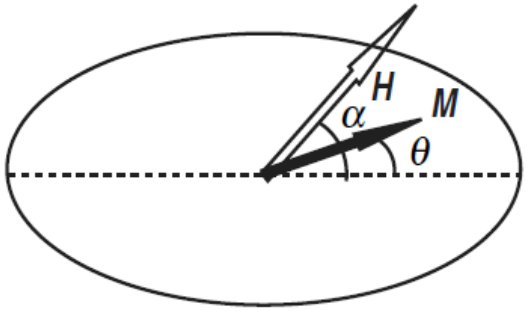

A Stoner–Wohlfarth particle.

$$E_{tot} = K_u \sin^2\theta - \mu_0 M H \cos(\alpha - \theta).$$

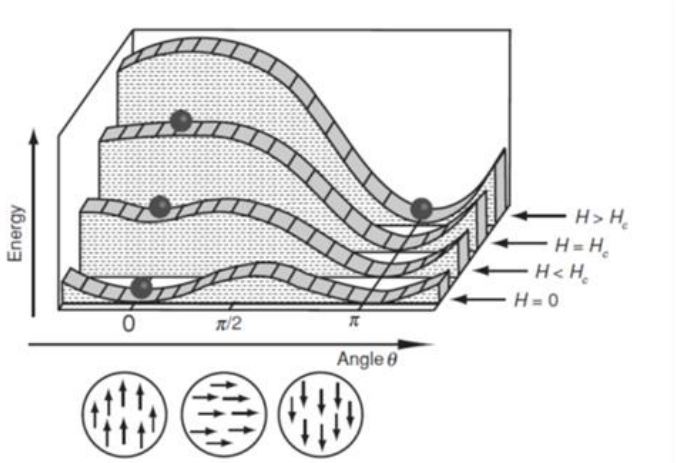

7.3.1 Stoner–Wohlfarth model

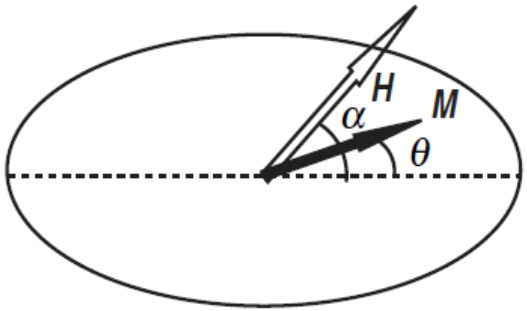

A Stoner–Wohlfarth particle.

$$E_{tot} = K_u \sin^2\theta - \mu_0 M H \cos(\alpha - \theta).$$

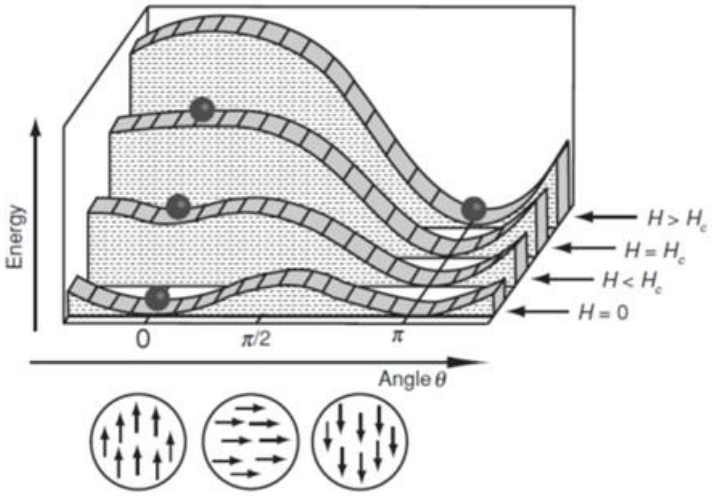

$$d^2E/d\theta^2 = 0$$

7.3.1 Stoner–Wohlfarth model

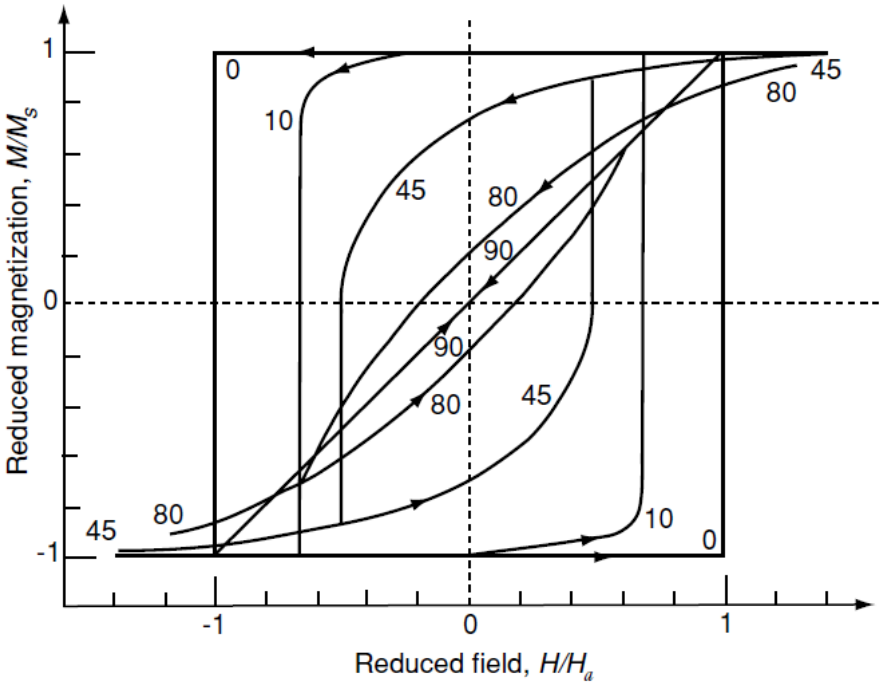

$\alpha < 45°$,

the switching field H_{sw} is then equal to the coercivity H_c

$\alpha > 45°$,

$H_{sw} > H_c$

The hysteresis loop is perfectly square when a = 0, and in that case the coercivity is equal to the anisotropy field:

$$H_c = 2K_u/\mu_0 M_s$$

$$H_c = (2K_1/\mu_0 M_s) + [(1 - 3\mathcal{N})/2]M_s$$

7.3.1 Stoner–Wohlfarth model

An array of noninteracting particles with a random distribution of anisotropy axes is a crude model for a real polycrystalline magnet.

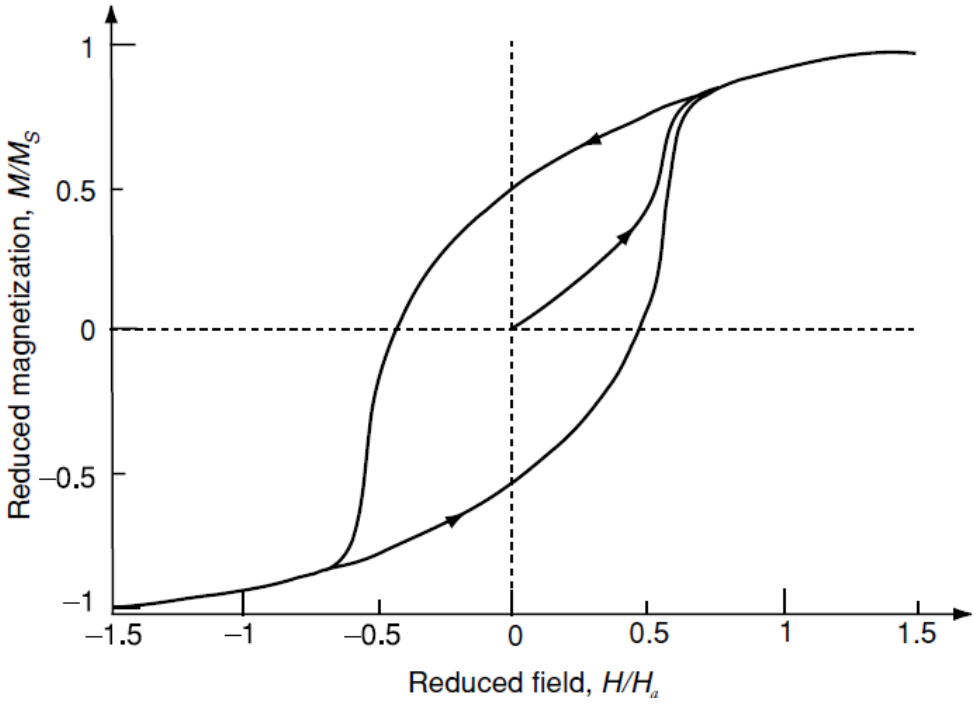

7.3.2 Reversal in thin films and small elements

The magnetization of soft ferromagnetic films usually lies in the plane of the film, in order to minimize the demagnetizing field.

A weak, in-plane uniaxial anisotropy Ku may be induced deliberately to control the reversal process by magnetic annealing or off-axis deposition.

The thin-film element is equivalent to a Stoner–Wohlfarth particle, for which the coherent rotation of the magnetization is confined to a plane.

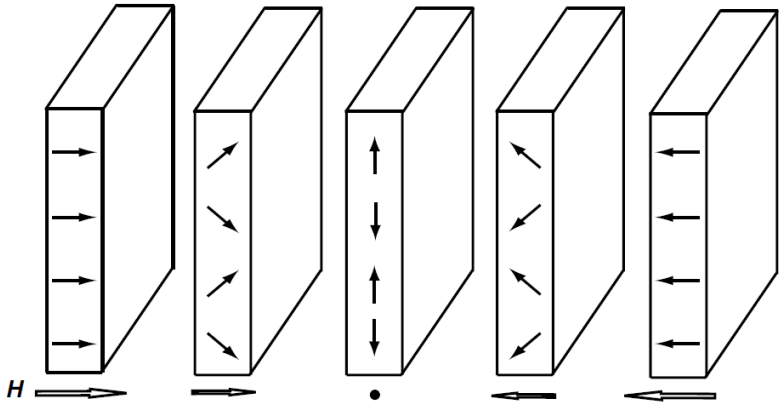

Coherent rotation of the magnetization is an assumption of the Stoner–Wohlfarth theory. It must be emphasized that other reversal modes may be possible, which have less coercivity.

7.3.2 Reversal in thin films and small elements

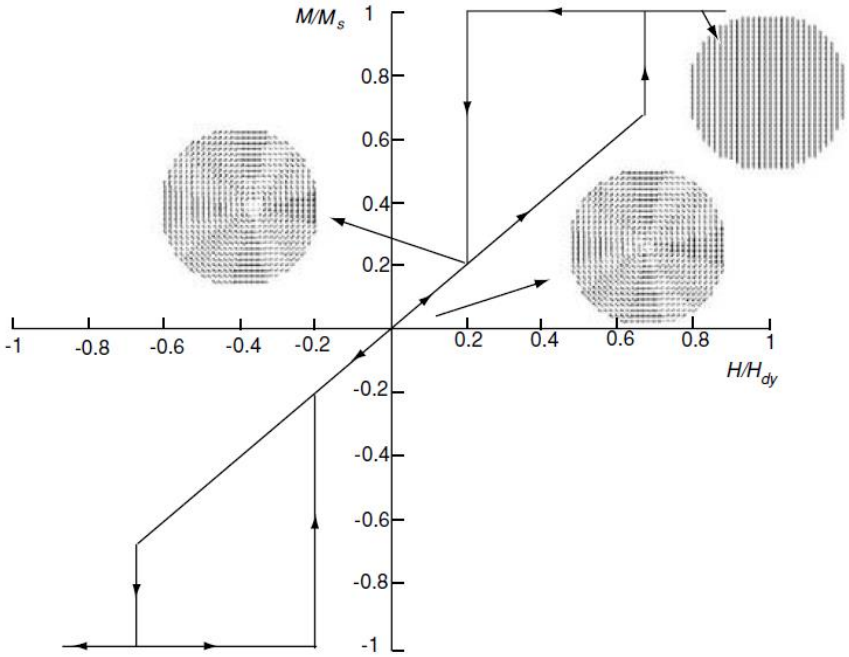

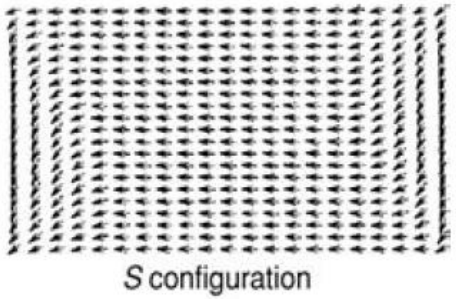
S configuration

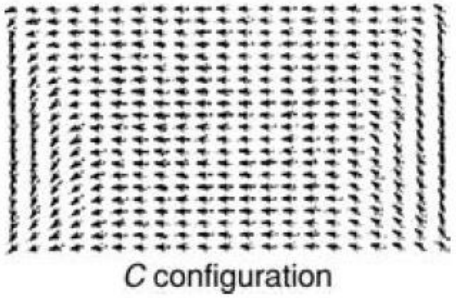
C configuration

Whereas small thin-film ferromagnetic elements tend to have a collinear structure and reverse coherently, as described by the Stoner–Wohlfarth model, larger elements with negligible anisotropy tend to adopt a vortex state. Acircular dot has four possible configurations, with clockwise or anticlockwise chirality and the spins at the centre can point up or down out of the plane. Starting from one of these, an in-plane field pushes the vortex reversibly towards the edge of the dot, and the magnetization then switches irreversibly to saturation

7.3.3 Perpendicular anisotropy

Perpendicular anisotropy can arise when an oriented or epitaxial film of a hard magnetic material is, grown with its easy axis perpendicular to the film plane.
In the very thinnest films a few nanometers thick, surface anisotropy can sometimes lead to perpendicular magnetization (§8.2.2).

Multilayer stacks with perpendicular anisotropy can be built up of alternating thin ferromagnetic and nonmagnetic layers.

If ϑ is the angle between the magnetization and the film normal, and there is some perpendicular anisotropy Ku, the energy per unit volume,

$$E_{tot} = K_u \sin^2 \vartheta + \tfrac{1}{2}\mu_0 M_s^2 \cos^2 \vartheta,$$

the condition for perpendicular anisotropy

$$K_u > \tfrac{1}{2}\mu_0 M_s^2$$

7.3.3 Perpendicular anisotropy

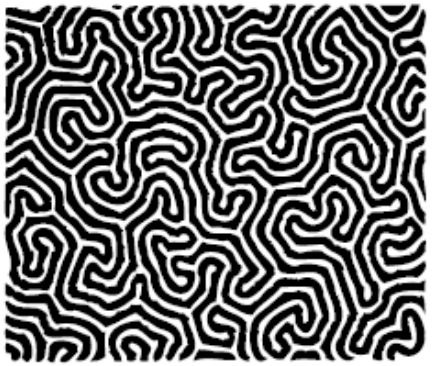

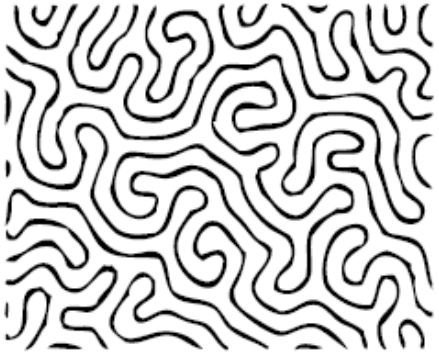

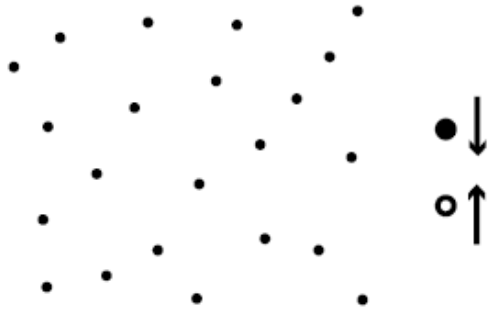

$H = 0$ $\odot H$ $\odot H$

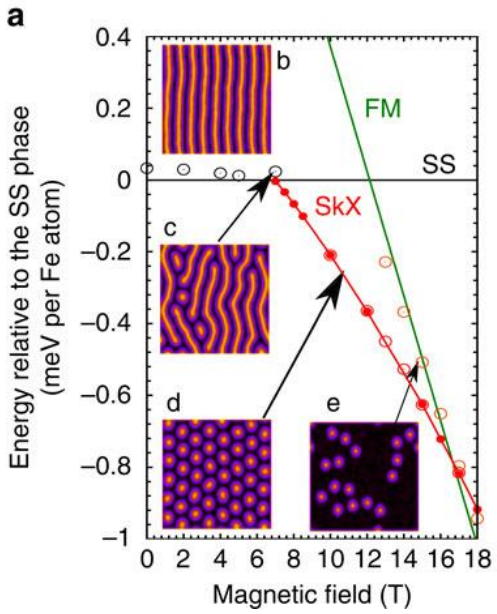

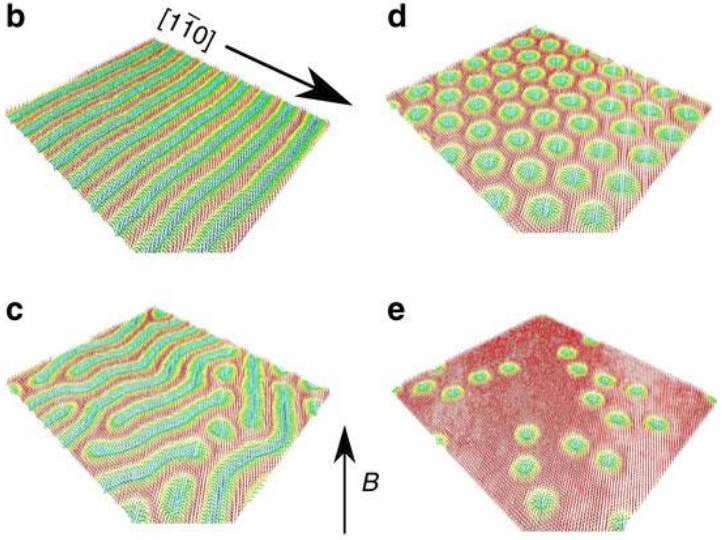

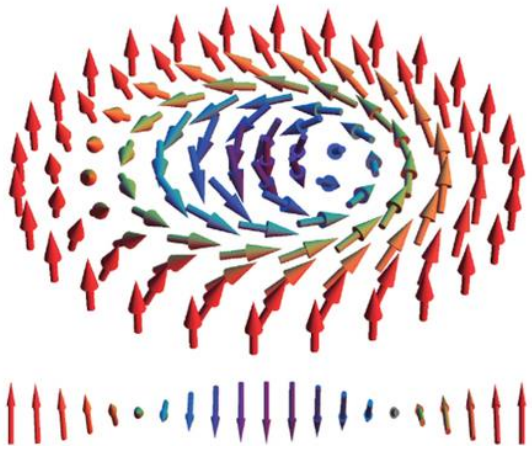

7.3.4 Nucleation

Starting from a uniformly magnetized ellispoidal sample, the nucleation field Hn is defined as the field where the first deviation from the uniformly magnetized state appears.

Coercivity is conventionally positive, whereas the nucleation field is negative.

Brown actually proved that

$$H_n \leq -2K_1/\mu_0 M_s + \mathcal{N} M.$$

Since nucleation must precede reversal,

$$H_c \geq -H_n$$

Nucleation of the coherent reversal mode is deduced from an eigenmode analysis of the linearized micromagnetic equation:

$$H_n = -\frac{2K_1}{\mu_0 M_s} - \frac{1}{2}(1 - 3\mathcal{N})M_s,$$

7.3.4 Nucleation

$$E_{tot} = K_u \sin^2\theta - \mu_0 M H \cos(\alpha - \theta).$$

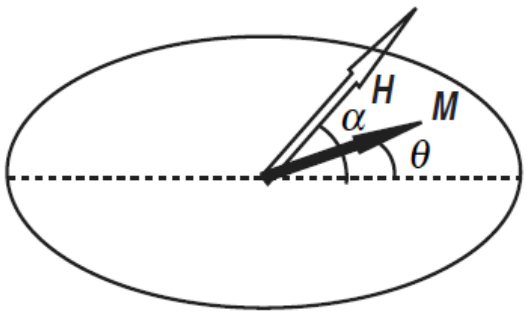

A Stoner–Wohlfarth particle.

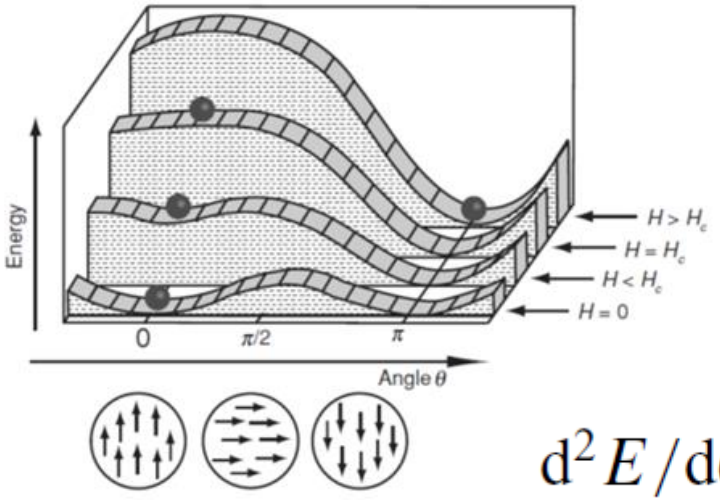

$$d^2E/d\theta^2 = 0$$

$$H_c = 2K_u/\mu_0 M_s$$

$$H_c = (2K_1/\mu_0 M_s) + [(1 - 3\mathcal{N})/2]M_s$$

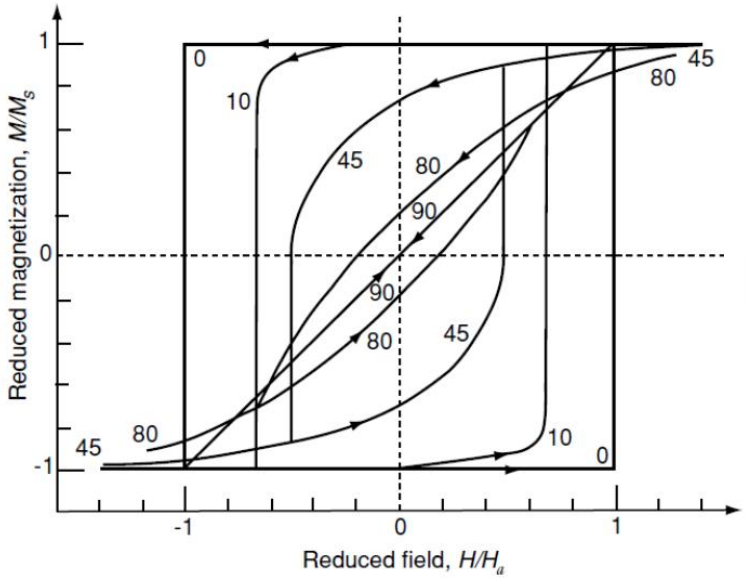

$$H_n = -\frac{2K_1}{\mu_0 M_s} - \frac{1}{2}(1 - 3\mathcal{N})M_s,$$

7.3.4 Nucleation

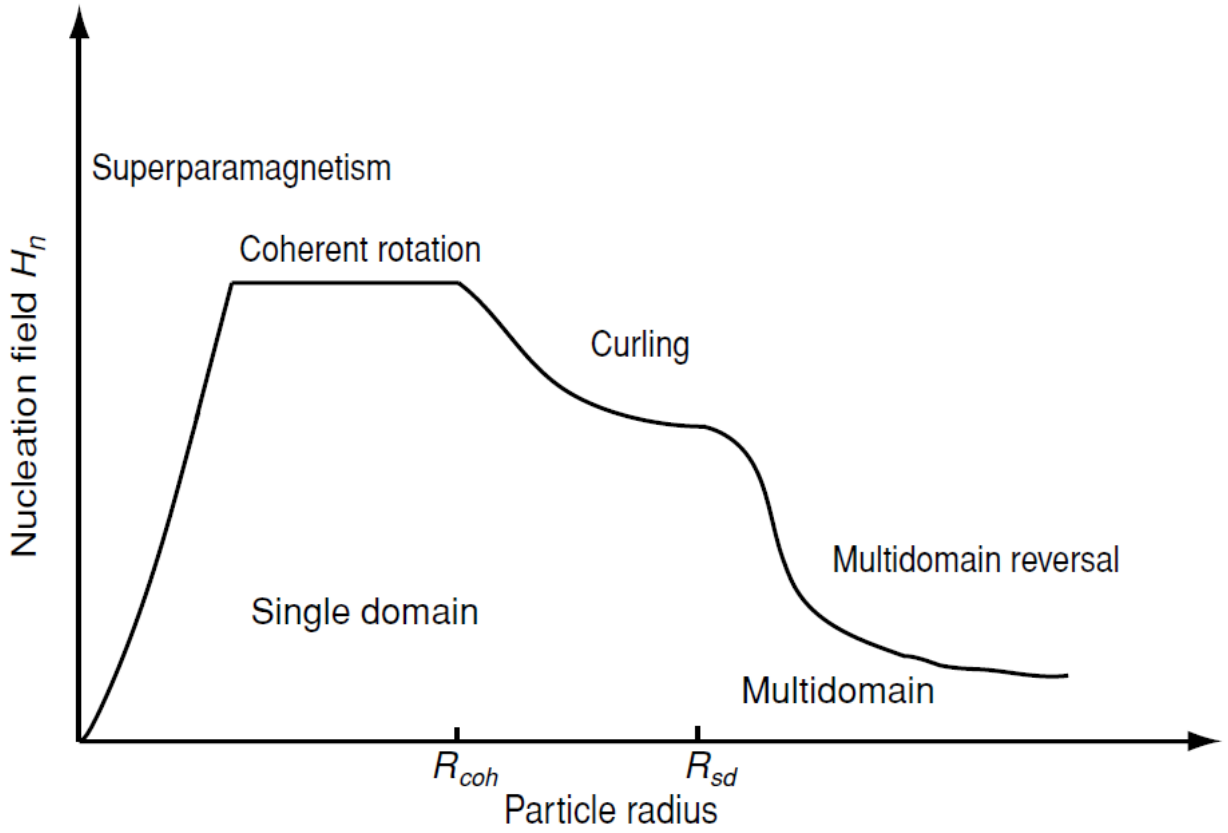

8.5.1 Superparamagnetism

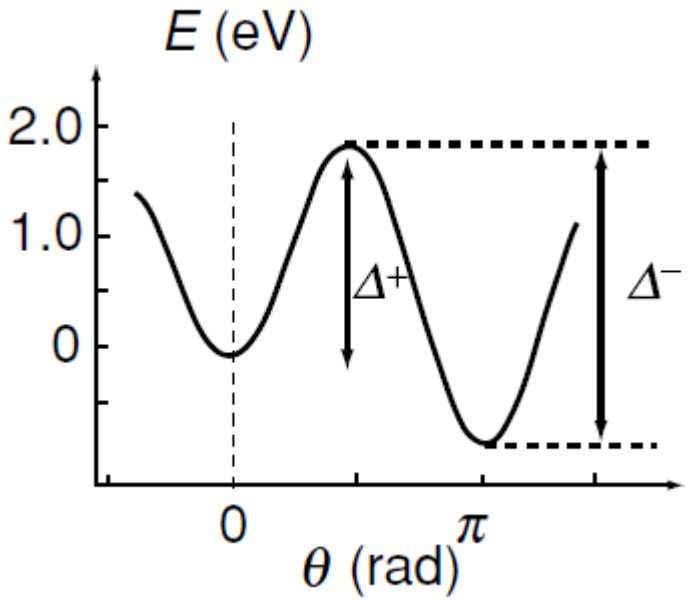

Tiny ferromagnetic particles of radius R ~10 nm become unstable when the energy barrier to magnetic reversal is comparable to $k_B T$

The spin-flip frequency

= an attempt frequency × the Boltzman probability

$$\tau_0^{-1} \qquad \exp(-\Delta/k_B T)$$

$$\Delta^{\pm} \Longrightarrow \Delta \pm \mu_0 \mathrm{m} H \cos\theta_0$$

the relaxation time for a spin flip

$$\tau = \tau_0 \exp(\Delta / k_B T),$$

$$\tau_0^{-1} \text{ is of order 1 GHz}$$

There is progressive, but exponentially rapid slowing down of the magnetic relaxation around some blocking temperature

$$T_b < T_C$$

8.5.1 Superparamagnetism

A commonly used criterion for blocking

$$\Delta / k_B T = 25$$

corresponds to $\tau \approx 100$ s which is about the time needed for a magnetic measurement.

Table 8.5. Superparamagnetic relaxation times for cobalt particles

Radius (mm)	Temperature (K)	Relaxation time
3.5	260	332 s
3.5	300	10 s
3.5	340	0.6 s
3.5	380	76 ms
3.0	300	1.9 ms
4.0	300	223 h
5.0	300	L $\times 10^{12}$ y

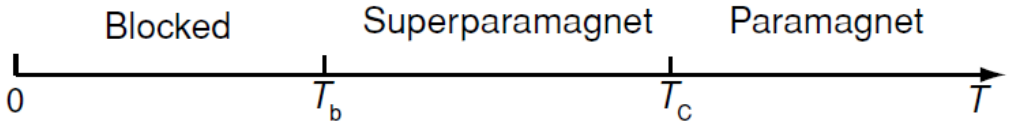

7.3.6 Switching dynamics

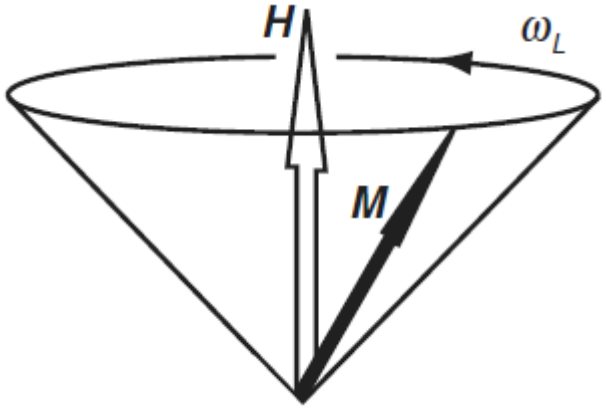

a torque $\boldsymbol{\Gamma} = \mu_0 \mathrm{m} \times \boldsymbol{H}$

$$\gamma = g\mu_B/\hbar$$

$$\mathrm{d}\boldsymbol{M}/\mathrm{d}t = \gamma\mu_0 \boldsymbol{M} \times \boldsymbol{H}$$

The Larmor precession or ferromagnetic resonance frequency

$$\omega_L = \gamma\mu_0 H$$

When there is uniaxial anisotropy, represented by an anisotropy field

$$H_a = \ 2K_1/\mu_0 M_s$$

$$\omega_L = \gamma\mu_0(H + H_a).$$

7.3.6 Switching dynamics

The Landau–Lifschitz–Gilbert equation

$$\mathrm{d}\boldsymbol{M}/\mathrm{d}t = \gamma\mu_0\boldsymbol{M}\times\boldsymbol{H} - (\alpha/M_s)\boldsymbol{M}\times\mathrm{d}\boldsymbol{M}/\mathrm{d}t$$

If the field is applied in the plane of a ferromagnetic film, perpendicular to the easy axis, the magnetization tries to precess out of the plane and it is then subject to a large demagnetizing field of order of a tesla, which accelerates the rotation of themagnetization towards the field

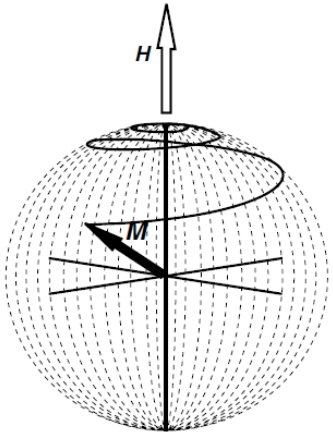

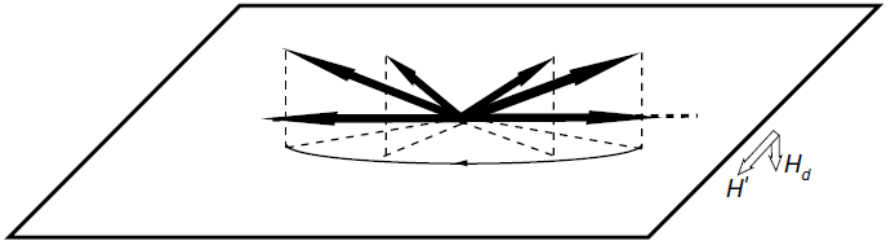

7.3.7 Domain-wall motion

Reversal involving domain-wall motion is far slower.
An applied field exerts a pressure on the walls.

If it is applied parallel to the easy z axis of a uniaxial magnet, the wall will move in the x-direction.
The change in Zeeman energy per unit area of wall is

$$2\mu_0 M H \delta x$$

hence the pressure is

$$2\mu_0 M H$$

the wall velocity is essentially proportional to the pressure:

$$v_w = \mu_0 \eta_w (H - H_p),$$

Mobilities range from 1 to 1000 m s^{-1} mT^{-1},

A field of 0.1 mT will move the walls at about 10 m s^{-1}.

7.3.7 Domain-wall motion

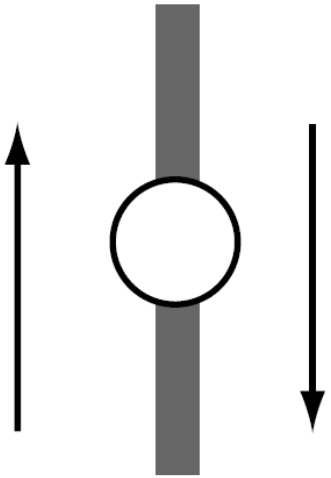

Domain wall pinned at a defect.

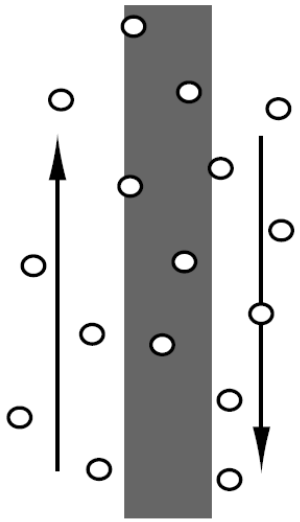

Weak pinning by multiple defects.

Strong pinning arises when these defects have a dimension comparable to the domain wall width δ_w

Weak pinning occurs when many small defects, particularly point defects, are distributed throughout the wall.
The energy for weak pinning derives from statistical fluctuations in the numbers of defects contained in the wall.

Inevitably, there will always be some distribution of defects in any sample of magnetic material.

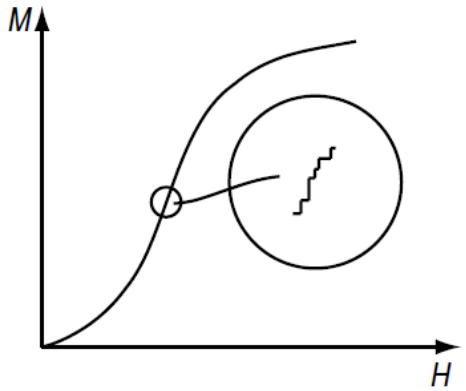

Barkhausen jumps.

7.3.8 Real hysteresis loops

Hysteresis loops in real materials exhibit features of nucleation, wall motion and coherent rotation.

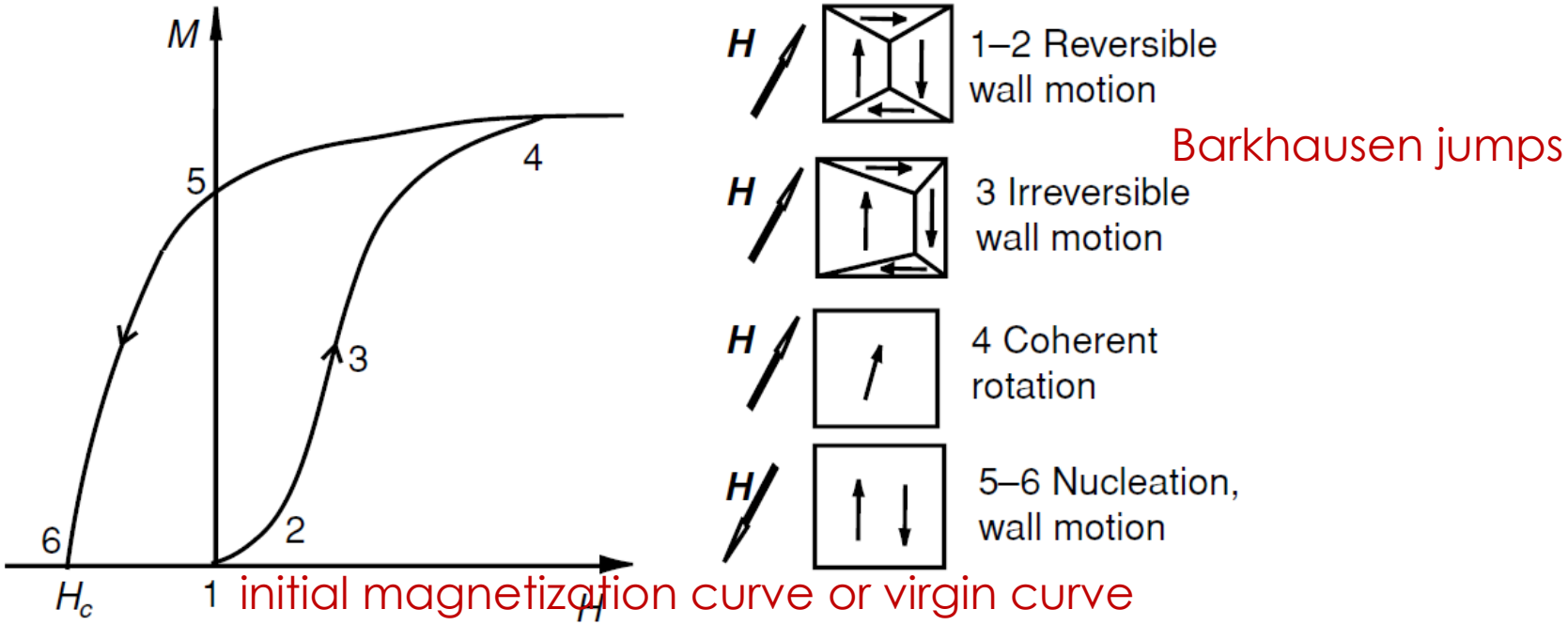

reverse domains nucleate and begin to propagate, eventually reducing the sample to a multidomain state with no net magnetization at the coercive field Hc. This multidomain state is a minimum in the energy landscape far removed from the virgin state 1, which is now forever inaccessible, unless the ferromagnet is reborn by heating above the Curie point, and cooling in zero field.

7.3.8 Real hysteresis loops

Hard magnetic materials whose magnetization process is governed by nucleation or pinning are readily distinguished by their initial magnetization curves.
The domain walls move freely through a nucleation-type magnet, which has a high initial susceptibility, but they are constantly being trapped in a pinning type magnet, so the initial susceptibility is small until the depinning field is reached.